

# UC Berkeley

## SEMM Reports Series

### Title

Large-Scale Modeling of Localized Dissipative Mechanisms in a Local Continuum:  
Applications to the Numerical Simulation of Strain Localization in Rate-Dependent Inelastic  
Solids

### Permalink

<https://escholarship.org/uc/item/3wz7z1hw>

### Author


Armero, Francisco

### Publication Date

1997-08-01

REPORT NO.  
UCB/SEMM-97/12

STRUCTURAL ENGINEERING  
MECHANICS AND MATERIALS



**LARGE-SCALE MODELING OF  
LOCALIZED DISSIPATIVE MECHANISMS  
IN A LOCAL CONTINUUM:  
APPLICATIONS TO THE  
NUMERICAL SIMULATION  
OF STRAIN LOCALIZATION IN  
RATE-DEPENDENT INELASTIC SOLIDS**

BY

**F. ARMERO**

AUGUST 1997

DEPARTMENT OF CIVIL AND ENVIRONMENTAL ENGINEERING  
UNIVERSITY OF CALIFORNIA, BERKELEY

# Large-Scale Modeling of Localized Dissipative Mechanisms in a Local Continuum: Applications to the Numerical Simulation of Strain Localization in Rate-Dependent Inelastic Solids

by

F. ARMERO

Structural Engineering, Mechanics and Materials  
Department of Civil and Environmental Engineering  
University of California, Berkeley CA 94720, USA  
armero@ce.berkeley.edu

## Abstract

This paper presents a general framework for the formulation of constitutive models that incorporate a localized dissipative mechanism. The formalism of strong discontinuities is employed, allowing for the decoupling of the constitutive characterization of the continuum and localized responses of the material. A procedure for incorporating the localized small scale effects of the material response in the large scale problem characterized by the standard local continuum is described in detail. The resulting large scale model is able to capture objectively the localized dissipation observed in localized failures of solids and structures. A localized viscous slip model is presented as a model example. The finite element implementation of the proposed formulation arises naturally as a local element enhancement of the finite element interpolations, with no regularization of the discontinuities. The above considerations are formulated first in the infinitesimal range, and then extended to the finite strain regime. Furthermore, it is shown that the proposed framework allows for the development of effective finite element methods capturing in the large scale the localized dissipation observed in the failure of rate-dependent materials, avoiding the resolution of small length scales associated to the localization bands in these regularized models. Several representative numerical simulations are presented to illustrate these ideas.

**KEY WORDS:** strain localization; strong discontinuities; viscoplasticity; large-scale regularization; finite element method.

## 1. Introduction

Highly localized patterns of the deformation in the form of bands are often observed preceding the failure of solids and structures. Characteristic examples are shear bands in metals (see e.g. NEEDLEMAN & TVERGAARD [1984], and references therein) and soils (see e.g. VARDOULAKIS [1978]), or the localization bands of cracking in brittle materials like concrete or rocks (see e.g. READ & HEGEMEIER [1984], and references therein), among many other representative articles. An overall softening response of the solid leading to its final failure is often observed accompanying this phenomenon. The small scale associated to these bands, compared to the large-scale response of the solid or structure, is to be noted. For example, shear bands of order of microns can be found in metals (BAI & DODD [1992]) or of order of millimeters (MUHLHAUS & VARDOULAKIS [1987]) in the case of soils, whereas characteristic lengths of typical applications are of the order of meters, or even kilometers in geological problems. In this way, the smooth pattern of the deformation of the solid previous to the appearance of strain localization gives rise to highly non-smooth solutions with *localized dissipative mechanisms* in the small scale, especially when observed from the large structural scale. The practical importance of capturing these localization modes while solving the large-scale (structural) problem is clear.

Classical (local) rate-independent constitutive models are known to lack an internal characteristic length, thus leaving undefined the small scales associated to the localized solution. Furthermore, the introduction of strain-softening in the local continuum is known to lead to inconsistencies in the resulting mechanical models. The classical work of THOMAS [1961], HILL [1962] and MANDEL [1966], and the more recent analyses in RICE [1976], OTTOSEN & RUNESSON [1991] and NEILSEN & SCHREYER [1993], among others, have identified the ill-posedness of problems involving a continuum with strain-softening. The leading part of the governing equations (the tangent operator) loses ellipticity, resulting in a change of type of the boundary value problem. The reader is referred also to the illustrative dynamic analysis of a one dimensional rod presented in BAZANT & BELYTSCHKO [1985]. Briefly, these inconsistencies can be traced back again to the lack of an internal characteristic length defining a material volume where the energy dissipation per unit volume imposed by a softening stress/strain relation can take place. As a consequence, the finite element solutions obtained in this context exhibit the well-known pathological dependence on the mesh size; see e.g. TVERGAARD et al. [1981], and PIETRUSZCZAK & MRÓZ [1981], among many others.

Mathematical analyses of the perfectly plastic rate-independent problem (see JOHNSON [1976], MATTHIES et al [1979], SUQUET [1981], and TEMAM [1984], among others) have identified the existence of non-smooth solutions involving discontinuous displacement fields, the so-called *strong discontinuities*, thus reproducing the highly non-homogeneous states of strain associated to the localized deformations. The observation that perfect plasticity defines a hyperbolic boundary value problem goes back to PRANDTL [1920], and leads to the classical slip line theory of rigid-plasticity. The slip lines define in this context

possible surfaces of discontinuity of the displacement field, identifying the failure mechanism of the solid; see e.g. the accounts in HILL [1950] or LUBLINER [1990], among others. The introduction of a localized dissipative mechanism along these discontinuities, through a stress/displacement relation as in the so-called discrete crack approaches of cracking in concrete (see HILLERBORG et al [1976]), is required for the proper characterization of the final localized failure of the material. The formulation of a general framework that incorporates these localized effects in the local continuum is the first objective of the present work.

The identification of these inconsistencies has motivated the formulation of many regularization techniques to avoid the associated difficulties. The main idea in these regularized formulations is the incorporation of internal length scales in the constitutive model. We can find along these lines the formulation of non-local models defining the constitutive relations at one point through the state of deformation in a finite neighborhood of it (see e.g. BAZANT et al [1984]); higher-gradient models incorporating higher order effects in the local constitutive relation, leading to higher order boundary value problems (see e.g. COLEMAN & HODGON [1985]); and the consideration of Cosserat continua accommodating rotational degrees of freedom and, hence, defining a length scale when related to the displacement field (see e.g. DEBORST & SLUYS [1991]), to mention just some few representative references.

Similarly, it is known that rate-dependent models introduce a length scale in the constitutive relation, even in the local continuum framework; see e.g. NEEDLEMAN [1988]. More precisely, the presence of a material viscosity defines a characteristic material time that together with the existence of a characteristic velocity in dynamic problems leads to the appearance of a length scale. The boundary-value problem remains well-posed (i.e., no change of type occurs). The onset of strain localization has been related in this case to the appearance of unstable (growing in time) modes in a spectral analysis of the linearized equations of motion. See MOLINARI & CLIFTON [1987] and references therein for complete details of these ideas. The well-posedness of the problem still holds in the quasi-static limit, but then the presence of imperfections highly influences the final localized solution. See NEEDLEMAN [1988] and BELYTSCHKO et al [1991], among others.

The common idea behind all these regularized approaches is the introduction of the small length scales characterizing the localized solutions. Consequently, the regularization will be effective if these small length scales are resolved by the tools employed in the analysis, e.g., the spatial discretization employed in their numerical simulation. The appropriateness of this approach is clear when the main objective is the understanding the details of the localized mechanisms that appear in the small scale of the material response. The multi-scale character of the problem needs to be brought up again. In this context, it may be difficult to motivate complex detailed analyses when the large-scale response of the structural system is the main objective. The issue is not only of computational cost, but also the appropriateness of maintaining standard formulations of the mechanical

problem in stages previous to the failure of the structure and in the large scale, away from the localized deformation patterns, where traditional numerical techniques are known to perform well.

The considerations above identify the need for the formulation of constitutive models that capture the localized dissipation observed in the failure of solids while maintaining the local continuum framework of the large scale. In this context, the goals of the work presented herein are twofold. The first objective is the formulation of a large-scale model that incorporates localized dissipative mechanisms, but treat the small scales associated to strain localization as unresolvable otherwise. The second goal is then the formulation of numerical methods (finite element methods, in particular) that implement these ideas and are able to capture these highly non-smooth solutions accurately. In particular, it is our goal to develop numerical techniques that capture effectively the localized dissipation of regularized rate-dependent models without the need of resolving the associated small length scales. One can talk in this last case of the “large-scale regularization of regularized models.”

Early attempts of the formulation of large-scale model capturing the localized dissipative effects can be traced back to smeared crack models of the cracking of concrete. See e.g. BAZANT & OH [1983] and ROTS et al [1985], among others. In this context, the formulation of continuum models capturing objectively the localized energy dissipation is accomplished through the proper definition of the softening law depending on the mesh size employed in the finite element analysis. In this way, the so-called *characteristic length* is introduced in the formulation of the mechanical model; see e.g. PIETRUSZCZAK & MRÓZ [1981] and OLIVER [1989]. Related approaches can be found in the formulation of finite elements involving a-priori defined internal length scales as in BELYTSCHKO et al [1988].

The analysis of strong discontinuities in inelastic continuum models has been presented in SIMO et al [1993], ARMERO & GARIKIPATI [1995,96], and OLIVER [1996]. The extension of these analyses to the finite strain range has been presented in ARMERO & GARIKIPATI [1996]. See also LARSSON & RUNESSON [1996] for a related approach involving a regularized discontinuity. The formulation of locally enhanced finite elements with regularized discontinuities can be found in SIMO et al [1993], and OLIVER [1996], with the limit case involving no regularization presented in ARMERO & GARIKIPATI [1995,96] for elastoplastic models, and ARMERO [1997] for damage models of cracking. Finite elements incorporating embedded localization lines have been also presented in DVORKIN et al. [1990]. The related approach presented in ORTIZ et al [1987] and NACAR et al [1989], involving also a local enhancement of the finite element interpolation with discontinuous displacements but with no added dissipative mechanism, can also be mentioned.

We present in this paper a general framework for the characterization of the dissipative mechanisms that appear in the failure of solids. The singular fields associated with strong discontinuities are introduced *locally* in a neighborhood of a continuum solid. This formalism allows a full decoupling of the characterization of the bulk and localized response of



the material. Both responses are then modeled independently, with the localized contributions involving a stress/displacement relation that dissipates energy objectively. No length scales are required at this stage. It is the incorporation of these local effects in the large-scale problem, involving smooth fields, that identifies the length scale characteristic of the problem. The limit of vanishing small scales (the large-scale limit) is then taken, leading to a large-scale model involving a local continuum that captures correctly the localized dissipation in the solid. Furthermore, this constructive incorporation of the small-scale effects in the large-scale problem allows not only for the simple numerical implementation of these ideas through a local enhancement of the finite element interpolations, but also for the formulation of the large-scale regularization of rate-dependent models. The numerical implementation of the latter involves the correct scaling of the localized dissipative mechanism along the strong discontinuity, thus capturing the proper dissipation depending on the degree of resolution of the small scales by the assumed spatial discretization. The developments considered herein focus on elastoplastic models characteristic of ductile materials, in both the infinitesimal and finite deformation ranges. The formulation of large-scale models incorporating the localized damage mechanism characteristic of brittle materials can be found in ARMERO [1997].

An outline of the rest of the paper is as follows. Section 2 describes the large-scale problem of interest in this work, consisting of the principle of virtual work with the standard regularity assumptions. The infinitesimal case is considered. Section 3 develops the constitutive modeling of localized dissipative mechanism in the small scale of the material characterized by a local neighborhood of a given material point. These mechanisms are characterized by the singular fields of strong discontinuities, with their constitutive modeling fully characterized in a thermodynamical framework based on the principle of maximum plastic dissipation. Section 4 effectively bridges the two problems, the small and large scale problems, leading in the large scale limit to a consistent formulation of the local continuum that captures the dissipative effects identified previously in the small scales. The proposed approach is then used for the formulation of the large-scale regularization of rate-dependent models in Section 4.2, and the formulation of finite element methods incorporating these ideas in Section 4.3. The extension of all these considerations to the finite strain range in Section 5. Representative numerical simulations are presented in Section 6 to assess the performance of the proposed finite element formulations. Finally, Section 7 concludes with some final remarks.

## 2. The Large-Scale Problem

This section summarizes the equations governing the large-scale mechanical problem, in the weak form of interest for the development of finite element methods as presented in Section 6. Regardless of the details particular to the constitutive model defined in Section 3, the equations for the large-scale problem as assumed in this section retain the usual smoothness properties.

Let a domain  $\Omega \subset \mathbb{R}^{n_{\text{dim}}}$  ( $n_{\text{dim}} = 1, 2$  or  $3$ ) define the reference placement of a solid body, identified with its current placement under the assumption of infinitesimal strains assumed in this section. Extensions to the finite deformation case are considered in Section 5. We denote by  $\mathbf{u} : \Omega \times [0, T] \rightarrow \mathbb{R}^{n_{\text{dim}}}$  the displacement field  $\mathbf{u}(\mathbf{x}, t)$  in a certain time interval  $T$ . This displacement field is imposed to satisfy the essential boundary conditions

$$\mathbf{u} = \bar{\mathbf{g}} \quad \text{on } \partial_u \Omega, \quad (2.1)$$

for some specified function  $\bar{\mathbf{g}}$  in part of the boundary  $\partial_u \Omega \subset \partial \Omega$ . We define the space of admissible displacement variations

$$\mathcal{V} = \left\{ \boldsymbol{\eta} : \Omega \rightarrow \mathbb{R}^{n_{\text{dim}}} : \boldsymbol{\eta} = 0 \quad \text{on } \partial_u \Omega \right\}, \quad (2.2)$$

that is, satisfying homogeneous boundary conditions on  $\partial_u \Omega$  where the displacement field is imposed. Standard regularity conditions are assumed for the displacement fields  $\boldsymbol{\eta} \in \mathcal{V}$ , the motivation being the tools of analysis available. In particular, the assumed large-scale fields can be easily resolved by standard techniques of finite element analysis, as illustrated in Section 4.3. Additional contributions due to the specific response of the material (e.g., discontinuities) are introduced in Section 3.

The infinitesimal *large-scale strains* are obtained as

$$\boldsymbol{\varepsilon}(\mathbf{u}) := \nabla^s \mathbf{u} := \frac{1}{2} [\nabla \mathbf{u} + (\nabla \mathbf{u})^T], \quad (2.3)$$

with  $(\cdot)^T$  denoting the matrix transpose. Let  $\boldsymbol{\sigma} = \boldsymbol{\sigma}(\mathbf{x}) \in \mathbb{R}^{n_{\text{dim}} \times n_{\text{dim}}}$  (symmetric) be the stress field in the solid. We denote the applied body force by  $\mathbf{b} : \Omega \rightarrow \mathbb{R}^{n_{\text{dim}}}$  (per unit mass) and the imposed boundary tractions by  $\bar{\mathbf{t}} : \partial_T \Omega \rightarrow \mathbb{R}^{n_{\text{dim}}}$  acting on the part  $\partial_T \Omega \subset \partial \Omega$  of the boundary of the solid. The usual assumptions

$$\partial_u \Omega \cap \partial_T \Omega = \emptyset \quad \text{and} \quad \overline{\partial_u \Omega \cup \partial_T \Omega} = \partial \Omega, \quad (2.4)$$

in each of the  $n_{\text{dim}}$  components of the displacement/traction are assumed for a well-posed problem. See Figure 3.1 for an illustration. Finally, we denote by  $\ddot{\mathbf{u}} := d^2 \mathbf{u} / dt^2$  and by  $\rho_o$  the acceleration and the reference density of the solid, respectively.

The large-scale problem of the mechanical initial boundary value problem can then be written as

**The Infinitesimal Large Scale Problem.** Find  $\mathbf{u} \in \mathcal{V} + \bar{\mathbf{g}}$  satisfying

$$\int_{\Omega} \rho_o \ddot{\mathbf{u}} \cdot \boldsymbol{\eta} \, d\Omega + \int_{\Omega} \boldsymbol{\sigma} : \nabla^s \boldsymbol{\eta} \, d\Omega = \int_{\Omega} \rho_o \mathbf{b} \cdot \boldsymbol{\eta} \, d\Omega + \int_{\partial_T \Omega} \bar{\mathbf{t}} \cdot \boldsymbol{\eta} \, d\Gamma \quad \forall \boldsymbol{\eta} \in \mathcal{V}, \quad (2.5)$$

where the stress field  $\boldsymbol{\sigma}$  is given by the constitutive model developed in the following section, and for given initial conditions  $\mathbf{u}(\mathbf{x}, 0) = \mathbf{u}_o(\mathbf{x})$  and  $\dot{\mathbf{u}}(\mathbf{x}, 0) = \mathbf{v}_o(\mathbf{x})$  in the displacements and velocities, respectively.  $\square$



A standard argument based on the weak form (2.5) of the equilibrium equations shows the continuity of tractions for a given orientation defined by a unit vector  $\mathbf{n}$ . Indeed, let  $\Gamma$  be a generic smooth *material* surface passing through a point  $\mathbf{x} \in \Omega$  with unit normal  $\mathbf{n}$ . Assume that the stress field  $\boldsymbol{\sigma}$  is smooth in each of the components that  $\Gamma$  defines in  $\Omega$ . Integration by parts of (2.5) under this assumption, and accounting for the internal surface  $\Gamma$  with unit normal  $\mathbf{n}$  at  $\mathbf{x} \in \Omega$  leads to the strong form of the balance of linear momentum equation and natural boundary conditions

$$\operatorname{div} \boldsymbol{\sigma} + \rho_0 \mathbf{b} = 0 \quad \text{in } \Omega \setminus \Gamma, \quad (2.6)$$

$$\boldsymbol{\sigma} \mathbf{n} = \bar{\mathbf{t}} \quad \text{on } \partial_T \Omega, \quad (2.7)$$

together with the local form of the equilibrium across  $\Gamma$  given by

$$[\boldsymbol{\sigma}] \mathbf{n} = 0. \quad (2.8)$$

where  $[\boldsymbol{\sigma}]$  denotes the jump in the stress. Therefore, we have the well-defined vector

$$\mathbf{T}_\Gamma := \boldsymbol{\sigma} \mathbf{n} \Big|_\Gamma, \quad (2.9)$$

the traction vector on  $\Gamma$  for all directions  $\mathbf{n}$ , where the restriction at  $\mathbf{x} \in \Gamma \subset \Omega$  is understood in this last formula.

### 3. Characterization of Localized Dissipative Mechanisms in the Local Continuum

The previous section introduced the large-scale problem leaving undefined the constitutive relation between the stress and the strain fields. The assumed regularity of the large-scale displacements and corresponding strains may not incorporate all the effects observed in the response of the material. In this context, the main goal of this section is the characterization of a localized dissipative mechanism characterized by a discontinuity in the displacement field, a *strong discontinuity*. As discussed in the introduction, the consideration of non-smooth solutions describing the localized response of the material may be of practical use, even if the solutions are smooth but close to the limit situation of a singular strain field. These ideas are developed further in Section 4 and illustrated in the numerical examples of Section 6.

#### 3.1. The kinematics of strong discontinuities

Let  $\Omega_x \subset \Omega$  be a local neighborhood of a material point  $\mathbf{x} \in \Omega$ , whose dimensions and full characterization will be detailed in Section 4. Our goal is to model the response of the material when it exhibits a localized dissipative mechanism at  $\mathbf{x}$ . As noted in

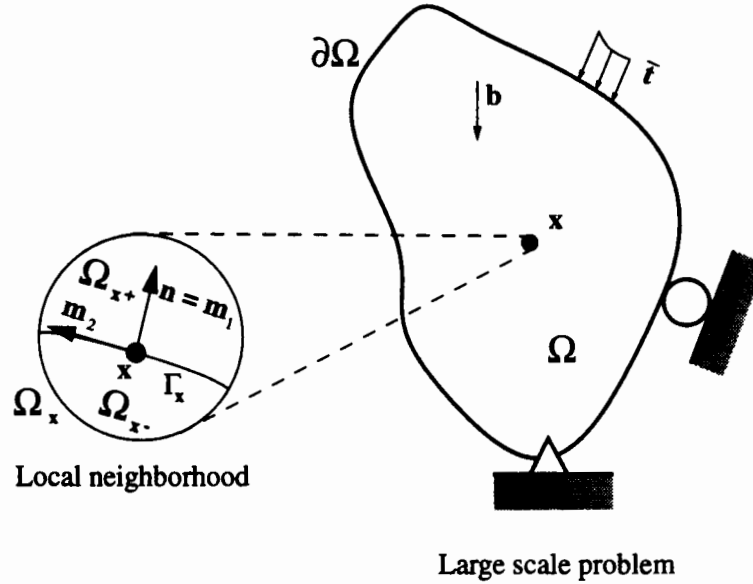


**FIGURE 3.1.** Large scale problem with standard boundary conditions. Definition of the local neighborhood  $\Omega_x \subset \Omega$  at a material point  $\mathbf{x}$ , with the smooth surface  $\Gamma_x$  and the corresponding orthogonal reference system  $\{\mathbf{m}_1 \equiv \mathbf{n}, \dots, \mathbf{m}_{n_{\text{dim}}}\}$  ( $n_{\text{dim}} = 2$  in the figure).

the introduction, we consider the large-scale limit characterized by the case of a strong discontinuity.

Assume the existence of a discontinuity in the displacement field across a surface  $\Gamma_x \subset \Omega_x$  passing through  $\mathbf{x} \in \Omega_x$  with unit normal  $\mathbf{n}$ . The discontinuous displacement field across the surface  $\Gamma_x$  can be written *locally in*  $\Omega_x$  using the decomposition

$$\mathbf{u}_\mu(\mathbf{y}) = \mathbf{u}(\mathbf{y}) + \xi(\mathbf{y}) M_{\Gamma_x}(\mathbf{y}) \quad \mathbf{y} \in \Omega_x, \quad (3.1)$$

where the function  $M_{\Gamma_x} : \Omega_x \rightarrow \mathbb{R}$  is smooth in  $\Omega_x \setminus \Gamma_x$  and is normalized to have a unit jump across the discontinuity  $\Gamma_x$ , that is,

$$[M_{\Gamma_x}] = 1 \quad \text{on } \Gamma_x. \quad (3.2)$$

Let  $H_{\Gamma_x}$  denote the Heaviside function across  $\Gamma_x$ , defined by

$$H_{\Gamma_x}(\mathbf{y}) = \begin{cases} 1 & \mathbf{y} \in \Omega_{x+}, \\ 0 & \mathbf{y} \in \Omega_{x-}, \end{cases} \quad (3.3)$$

where  $\Omega_{x+}$  and  $\Omega_{x-}$  denote each of the two connected components of the neighborhood  $\Omega_x$  defined by  $\Gamma_x$ ; see Figure 3.1. Given the definition (3.3) of the Heaviside function, the function  $M_{\Gamma_x}$  can be written

$$M_{\Gamma_x} = H_{\Gamma_x} + N_x, \quad (3.4)$$

for some smooth function  $N_x$  in  $\Omega_x$ . We note that no compatibility requirements between the displacement fields  $\mathbf{u}$  and  $\mathbf{u}_\mu$  are imposed a-priori on the local decomposition (3.1). The decomposition (3.1) is characteristic of the approach presented in SIMO et al [1993].

With these considerations the jump across  $\Gamma_x$  is given by

$$[\mathbf{u}_\mu] = \boldsymbol{\xi} . \quad (3.5)$$

For later use, we introduce the space of displacement jumps

$$\mathcal{J} = \{ \boldsymbol{\xi} : \Omega_x \rightarrow \mathbb{R}^{n_{\text{dim}}} \} , \quad (3.6)$$

a smooth extension in  $\Omega_x$  of the displacement jump  $\boldsymbol{\xi}_x$  at  $\mathbf{x}$  (i.e.,  $\boldsymbol{\xi}_x = \boldsymbol{\xi}(\mathbf{x})$ ). The displacement field  $\mathbf{u}_\mu : \Omega_x \rightarrow \mathbb{R}^{n_{\text{dim}}}$  defines the displacements observed locally in the small scale around the material point  $\mathbf{x}$ , incorporating the localized effects of the assumed discontinuous solution.

The infinitesimal strains corresponding to the displacement (3.1) are given by

$$\boldsymbol{\varepsilon}_\mu := \nabla^s \mathbf{u}_\mu = \underbrace{\boldsymbol{\varepsilon}(\mathbf{u}) + \boldsymbol{\xi} \otimes \nabla^s N_x + \nabla^s \boldsymbol{\xi} H_{\Gamma_x}}_{\text{regular distribution}} + \underbrace{(\boldsymbol{\xi} \otimes \mathbf{n})^s \delta_{\Gamma_x}}_{\text{singular distribution}} \quad \text{in } \Omega_x , \quad (3.7)$$

where the superscript  $s$  denotes the symmetric part. The singular part is expressed in terms of the singular distribution  $\delta_{\Gamma_x}$ , the Dirac delta across  $\Gamma_x$ . See STAKGOLD [1979] (page 100) for the mathematical details involved in the derivation of (3.7) from (3.1). We define

$$\bar{\boldsymbol{\varepsilon}}_\mu := \boldsymbol{\varepsilon}(\mathbf{u}) + (\boldsymbol{\xi} \otimes \nabla N_{\Gamma_x})^s + \nabla^s \boldsymbol{\xi} H_{\Gamma_x} \quad \text{in } \Omega_x , \quad (3.8)$$

for the regular part of  $\boldsymbol{\varepsilon}_\mu$ , and the singular strains

$$\tilde{\boldsymbol{\varepsilon}}_\delta := (\boldsymbol{\xi} \otimes \mathbf{n})^s \quad \text{on } \Gamma_x . \quad (3.9)$$

With this notation, the strains (3.7) in  $\Omega_x$  are given by

$$\boldsymbol{\varepsilon} = \bar{\boldsymbol{\varepsilon}}_\mu + \tilde{\boldsymbol{\varepsilon}}_\delta \delta_{\Gamma_x} . \quad (3.10)$$

Alternatively, the total strains  $\boldsymbol{\varepsilon}_\mu$  in  $\Omega_x$  can be decomposed as

$$\boldsymbol{\varepsilon}_\mu = \boldsymbol{\varepsilon}(\mathbf{u}) + \underbrace{\bar{\boldsymbol{\varepsilon}}_{unres} + \tilde{\boldsymbol{\varepsilon}}_\delta \delta_{\Gamma_x}}_{:= \boldsymbol{\varepsilon}_{unres}} . \quad (3.11)$$

where

$$\bar{\boldsymbol{\varepsilon}}_{unres} := \mathbf{G}(\boldsymbol{\xi}) := \bar{\boldsymbol{\varepsilon}}_\mu - \boldsymbol{\varepsilon}(\mathbf{u}) = (\boldsymbol{\xi} \otimes \nabla N_{\Gamma_x})^s + \nabla^s \boldsymbol{\xi} H_{\Gamma_x} \quad \text{in } \Omega_x . \quad (3.12)$$

Physically, the strain field  $\boldsymbol{\varepsilon}_{unres}$  is the part of the strains in  $\Omega_x$  which is *unresolved* by the strains  $\boldsymbol{\varepsilon}(\boldsymbol{u})$  considered in the large-scale problem. The decomposition (3.11) identifies the regular and singular part of these unresolved strains. Therefore, the unresolved strains (3.12) are given by

$$\boxed{\boldsymbol{\varepsilon}_{unres} = \boldsymbol{G}(\boldsymbol{\xi}) + (\boldsymbol{\xi} \otimes \boldsymbol{n})^s \delta_{\Gamma_x}}, \quad (3.13)$$

being a linear function of the displacement jumps  $\boldsymbol{\xi}$ .

### 3.2. The localized dissipation

Given the kinematics of the strong discontinuities described in the previous section, we consider the following dissipation functional

$$\mathcal{D}_\mu := \int_{\Omega_x} \left[ \boldsymbol{\sigma} : \dot{\boldsymbol{\varepsilon}}_\mu - \dot{W} \right] d\Omega_x, \quad (3.14)$$

in the local neighborhood  $\Omega_x$ , for a *stored energy function*

$$W = \hat{W}(\boldsymbol{\varepsilon}_\mu, \mathcal{I}), \quad (3.15)$$

in terms of the small-scale strains  $\boldsymbol{\varepsilon}_\mu$  and a set of internal variables  $\mathcal{I}$  to be specified. Uncoupled thermal conditions are assumed for simplicity (e.g. isothermal conditions with  $W$  corresponding to the free energy of the material). Our goal is the complete characterization of a localized dissipative mechanism along  $\Gamma_x$ . To this purpose, we assume the following constitutive decomposition of the stored energy in  $\Omega_x$

$$\boxed{W = \bar{W}(\bar{\boldsymbol{\varepsilon}}_\mu, \bar{\mathcal{I}}) + \tilde{W}(\boldsymbol{\xi}, \tilde{\mathcal{I}}) \delta_{\Gamma_x}}, \quad (3.16)$$

that is, we assume that the stored energy function of the material can be decomposed in a regular part  $\bar{W}$  in  $\Omega_x \setminus \Gamma_x$  and a singular part  $\tilde{W}$  on  $\Gamma_x$ , depending respectively on the regular and singular parts of the small-scale strains as defined by (3.10) and internal variables. In this way, the generic internal variables  $\bar{\mathcal{I}}$  characterize a bulk inelastic response in  $\Omega_x$ , whereas its singular counterparts  $\tilde{\mathcal{I}}$  do so along the discontinuity  $\Gamma_x$ . We observe that the main consequence of assumption (3.16) is the decoupling of the response of the continuum and the localized dissipative mechanism. This decoupling allows a separate characterization of both deformation responses as described next.

The introduction of the decomposition (3.16) in (3.14) together with the decomposition (3.7) of the strains leads to the final expression of the dissipation functional

$$\mathcal{D}_\mu = \int_{\Omega_x} \underbrace{\left[ \boldsymbol{\sigma} : \dot{\boldsymbol{\varepsilon}}_\mu - \dot{W} \right]}_{:= \bar{\mathcal{D}}_\mu} d\Omega_x + \int_{\Gamma_x} \underbrace{\left[ \boldsymbol{T} \cdot \dot{\boldsymbol{\xi}} - \dot{\tilde{W}} \right]}_{:= \tilde{\mathcal{D}}_\mu} d\Gamma_x, \quad (3.17)$$

after using the relation

$$\int_{\Omega_x} \boldsymbol{\sigma} : (\boldsymbol{\gamma} \otimes \mathbf{n})^s \delta_{\Gamma_x} d\Omega_x = \int_{\Gamma_x} \mathbf{T} \cdot \boldsymbol{\gamma} d\Gamma_x \quad \forall \boldsymbol{\gamma} \in \mathcal{J}, \quad (3.18)$$

defining the vector field  $\mathbf{T}$  on  $\Gamma_x$  in the small scale  $\Omega_x$ . Clearly, a completely decoupled expression of the dissipation is obtained, accounting for the contributions of the continuum and localized dissipative mechanisms, respectively. As expected, the latter is given by the difference between the power done by the tractions  $\mathbf{T}$  on the jump displacement rates  $\dot{\boldsymbol{\xi}}$  and the change in the stored energy of the localized dissipative mechanism  $\dot{\bar{W}}$ .

The characterization of the constitutive equations in the bulk of the material follows standard arguments based on the dissipation functional  $\bar{\mathcal{D}}_\mu$ , after the decoupling of the localized dissipative mechanism. For example, (visco) elastoplastic models can be found developed to all the extent in SIMO & HUGHES [1997]. We proceed in the next section with a similar characterization of the localized dissipative mechanism.

### 3.3. The localized constitutive relations

We develop in this section an elastoplastic model of the localized dissipative mechanism identified in the previous section. As shown in Section 3.3.1, this framework is appropriate for the modeling of strain localization in ductile materials. The reader is referred to ARMERO [1997] for the case of a localized anisotropic damage mechanism in the study of cracking of brittle materials.

A general elastoplastic model of the localized dissipative mechanism on  $\Gamma_x$  can be characterized by the additive decomposition of the displacement jumps

$$\boldsymbol{\xi} = \boldsymbol{\xi}^e + \boldsymbol{\xi}^p, \quad (3.19)$$

in elastic and plastic parts, respectively. Furthermore, we assume that the localized strain energy  $\bar{W}$  is a function of the elastic (or reversible) part of the displacement jump

$$\bar{W} = \bar{W}(\boldsymbol{\xi}^e, \bar{\alpha}), \quad (3.20)$$

where we have introduced a single scalar variable  $\bar{\alpha}$  to model the evolution of the irreversible processes along  $\Gamma_x$  for simplicity in the exposition that follows, and without loss of generality. The general case involving a different set of internal variables,  $\bar{\mathcal{I}}$  as in (3.16), follows easily. Note that  $\bar{\mathcal{I}} = \{\boldsymbol{\xi}^p, \bar{\alpha}\}$  in (3.20). The introduction of the stored energy (3.20) in the localized dissipation (3.17)<sub>2</sub> leads to the expression

$$\bar{\mathcal{D}}_\mu = \left( \mathbf{T} - \frac{\partial \bar{W}}{\partial \boldsymbol{\xi}^e} \right) \cdot \dot{\boldsymbol{\xi}}^e + \mathbf{T} \cdot \dot{\boldsymbol{\xi}}^p - \frac{\partial \bar{W}}{\partial \bar{\alpha}} \dot{\bar{\alpha}}. \quad (3.21)$$

Following standard arguments known as Coleman's method (see e.g. TRUESDELL & NOLL [1965]), that is, imposing the physically motivated constraint

$$\bar{\mathcal{D}}_\mu \geq 0, \quad (3.22)$$

for all processes and, in particular, for arbitrary changes of the reversible part  $\xi^e$  of the displacement jumps, we arrive at the localized constitutive relation for the traction vector

$$\mathbf{T} = \frac{\partial \bar{W}}{\partial \xi^e}, \quad (3.23)$$

and the final expression of the localized dissipation

$$\bar{\mathcal{D}}_\mu = \mathbf{T} \cdot \dot{\xi}^p + q \dot{\bar{\alpha}}. \quad (3.24)$$

The notation

$$q = -\frac{\partial \bar{W}}{\partial \bar{\alpha}}, \quad (3.25)$$

has been introduced in (3.24) for the stress-like internal variable  $q$ .

The localized elastoplastic response can be characterized then by a yield surface

$$\bar{\phi} = \bar{\phi}(\mathbf{T}, q), \quad (3.26)$$

depending on the thermodynamical forces  $\mathbf{T}$  and  $q$  conjugate to the rate of internal variables, as identified by the expression of the localized dissipation (3.24). The maximization of the dissipation functional (3.24) constrained by the yield condition  $\bar{\phi} \leq 0$  leads to the plastic evolution equations for the rate-independent case. Following e.g. SIMO & HUGHES [1997] we construct the unconstrained function

$$\bar{\mathcal{L}}_\mu(\mathbf{T}, q) := -\bar{\mathcal{D}}_\mu(\mathbf{T}, q) + \bar{\gamma} \bar{\phi}(\mathbf{T}, q), \quad (3.27)$$

for a (localized) consistency parameter  $\bar{\gamma}$  satisfying the Kuhn-Tucker loading/unloading conditions

$$\bar{\phi} \leq 0, \quad \bar{\gamma} \geq 0, \quad \text{and} \quad \bar{\gamma} \bar{\phi} = 0, \quad (3.28)$$

and the consistency condition

$$\bar{\gamma} \dot{\bar{\phi}} = 0. \quad (3.29)$$

The minimization of  $\bar{\mathcal{L}}_\mu$  for given rates  $\dot{\xi}^p$  and  $\dot{\bar{\alpha}}$  leads to the associated plastic evolution equations

$$\left. \begin{aligned} \dot{\xi}^p &= \bar{\gamma} \frac{\partial \bar{\phi}}{\partial \mathbf{T}}, \\ \dot{\bar{\alpha}} &= \bar{\gamma} \frac{\partial \bar{\phi}}{\partial q}, \end{aligned} \right\} \quad (3.30)$$



A Perzyna-type viscous regularization is obtained by replacing the Kuhn-Tucker loading/unloading conditions (3.28) and the consistency relation (3.29) by the evolution equation

$$\tilde{\gamma} = \frac{\langle g(\tilde{\phi}) \rangle}{\eta_L}, \quad (3.31)$$

for a localized viscous material parameter  $\eta_L$ , general scalar function  $g(\cdot)$ , and Macaulay brackets  $\langle \cdot \rangle^*$  while retaining the evolution equations (3.30).

In conclusion, the consideration of strong discontinuities in a local neighborhood of the local continuum allows for a complete characterization of the bulk and localized responses of the material. In both cases, the variational structure given by the principle of maximum internal dissipation can be used for the modeling of the corresponding inelastic effects. We present in the following section the example furnished by a rigid (visco)plastic slip model. Still, the above developments have been developed in the local neighborhood  $\Omega_x$ . The inclusion of the resulting localized constitutive model is undertaken in Section 4.

**Remark 3.1.** The above developments assumed a given unit normal  $\mathbf{n}$  to the discontinuity surface  $\Gamma_x$ . For the rate-independent limit, this normal is defined by the loss of ellipticity condition of the underlying continuum model; see e.g. SIMO et al [1993] and references therein. For rate-dependent solids, a case of special interest herein, it is known that the problem remains elliptic; see e.g. NEEDLEMAN [1988]. In particular, no strong discontinuities will appear. As noted in the introduction, and illustrated in Section 6, we still consider the limit situation defined by a strong discontinuity as an efficient mechanism to model and capture the localized dissipative mechanism associated to the onset of strain localization, without the need of resolving the corresponding small length scales. The numerical simulations presented in Section 6 consider a Perzyna-type viscoplastic  $J_2$ -flow theory model (see e.g. SIMO & HUGHES [1997]). In this context, we make use the result presented in LEROY & ORTIZ [1990] which indicates that a lower-bound for the appearance of strain localization in a rate-dependent model is obtained by considering the loss of ellipticity of the underlying rate-independent limit. The argument is based on a spectral analysis of the linearized governing equations, as studied in detail in e.g. MOLINARI & CLIFTON [1987], among others. The normal  $\mathbf{n}$  is then obtained as the zero eigenvector of the corresponding rate-independent acoustic tensor. This approach is employed in NACAR et al [1989] for the enhancement of finite elements. Note that the formulation proposed in this last reference does not incorporate a dissipative mechanism along the assumed discontinuities, in contrast with the approach proposed herein.  $\square$

---

\*  $\langle x \rangle := \begin{cases} 0 & \text{if } x \leq 0 \\ x & \text{if } x \geq 0 \end{cases}$

### 3.3.1. Model example: a rigid (visco)plastic slip model

We consider in this section the model example of a rigid-plastic slip model as it is observed in the strong discontinuities resulting from the analysis of continuum models of the  $J_2$ -flow theory of plasticity (see ARMERO & GARIKIPATI [1995,96] for details). The extension accommodating a viscous response is developed as well.

To this purpose, the rigid response is characterized by the lack of reversible displacement jumps

$$\boldsymbol{\xi}^e \equiv 0 \quad \Longrightarrow \quad \boldsymbol{\xi}^p \equiv \boldsymbol{\xi}, \quad (3.32)$$

so the localized stored energy function  $\bar{W}$  is simply given in terms of the scalar internal variable  $\bar{\alpha}$

$$\bar{W}(\boldsymbol{\xi}, \bar{\alpha}) = \mathcal{H}(\bar{\alpha}), \quad (3.33)$$

for some scalar function  $\mathcal{H}(\cdot)$  defining the cohesive opening of the discontinuity  $\Gamma_x$ . The localized slipping mechanism is characterized by the slip surface

$$\bar{\phi}(\mathbf{T}, q) = \|\mathbf{T}_T\| + q - \tau_y, \quad (3.34)$$

where  $\tau_y$  is the initial shear stress upon activation of the localized slip mechanism, and  $\|\mathbf{T}_T\|$  denotes the Euclidean norm of the tangential component of the traction vector, defined by

$$\mathbf{T}_T = \sum_{\beta=2}^{n_{\text{dim}}} T_\beta \mathbf{m}_\beta \quad \text{with} \quad T_\beta := \mathbf{T} \cdot \mathbf{m}_\beta \quad \text{and} \quad \|\mathbf{T}_T\|^2 := \sum_{\beta=2}^{n_{\text{dim}}} (T_\beta)^2, \quad (3.35)$$

for an orthonormal basis  $\{\mathbf{m}_1 \equiv \mathbf{n}, \dots, \mathbf{m}_{n_{\text{dim}}}\}$  (see Figure 3.1). A softening law (3.25) is considered, with

$$q = \hat{q}(\bar{\alpha}) := -\frac{d\mathcal{H}}{d\bar{\alpha}} \in [0, -\tau_y], \quad (3.36)$$

describing the irreversible response along the discontinuity. The general plastic evolution equations (3.30) read in this case

$$\left. \begin{aligned} \dot{\xi}_\beta &= \tilde{\gamma} \frac{T_\beta}{\|\mathbf{T}_T\|} \quad (\beta = 2, n_{\text{dim}}), \\ \dot{\xi}_1 &= 0, \\ \dot{\bar{\alpha}} &= \tilde{\gamma}, \end{aligned} \right\} \quad (3.37)$$

for the displacement jump components

$$\xi_1 := \boldsymbol{\xi} \cdot \mathbf{n} \quad \text{and} \quad \xi_\beta := \boldsymbol{\xi} \cdot \mathbf{m}_\beta, \quad (3.38)$$

together with the Kuhn-Tucker loading/unloading conditions (3.28) and consistency condition (3.29) for the rate-independent case, or the Perzyna viscous regularization (3.31)

for the viscous case. The connections with classical Schmid models of micromechanics are to be noted (see e.g. ASARO [1983]). Note that in this rigid case ( $\xi^e \equiv 0$ ) the relation (3.23) does not hold, and the traction  $\mathbf{T}$  on  $\Gamma_x$  can only be defined in terms of equilibrium considerations as described in the next section.

## 4. The Construction of the Local Continuum Formulation

As discussed in Section 2, we consider the large-scale problem governing the evolution of the solid under the standard regularity conditions for the different fields of interest, including the large-scale displacements  $\mathbf{u}$  and stresses  $\boldsymbol{\sigma}$ . The developments in Section 3 characterize completely the localized dissipative mechanism that may appear in the limit case of a strong discontinuity. It is important to emphasize that the arguments presented in these developments did not consider any length scale parameter. However, the arguments were developed locally in a fixed neighborhood  $\Omega_x$  of the material point  $\mathbf{x} \in \Omega$ , the small-scale problem, when our main interest is the solution of the large-scale problem described in Section 2. These two problems have been disconnected to all practical purposes.

The goal of this section is to connect these two problems by introducing the local constitutive model developed in Section 3 in the large-scale problem as defined in Section 2. In particular, this step identifies the length scales that appear in the problem. The limit case as  $measure(\Omega_x) \rightarrow 0$  is considered leading to the final formulation involving a local continuum. Section 4.2 presents the application of these developments for the large-scale regularization of rate-dependent constitutive models. The finite element implementation of these ideas is summarized in Section 4.3.

### 4.1. The final governing equations

The framework developed in the previous sections led to the development of the constitutive relations for the continuum in the local neighborhood  $\Omega_x$  and the localized dissipative mechanism on the discontinuity  $\Gamma_x$  independently. In particular, the tractions  $\mathbf{T}$  appearing in the localized constitutive relations were defined by the weak relations (3.18) on  $\Gamma_x$ , but otherwise unrelated to the stress field  $\boldsymbol{\sigma}$  in  $\Omega_x/\Gamma_x$ . We note also that the local neighborhood  $\Omega_x$  has not been specified. For the case of a fixed and finite neighborhood, the resulting formulation defines a non-local relation of the constitutive variables  $\boldsymbol{\xi}$ , as it is characteristic of the non-local constitutive models as proposed in BAZANT et al [1984], among others. As noted in the introduction, our goal is the development of a formulation that maintains the local continuum structure (i.e., the neighborhood  $\Omega_x$  is to be considered in the limit as  $measure(\Omega_x) \rightarrow 0$ ), and it is therefore consistent with the large-scale problem described in Section 2. In particular, the large-scale problem defines the local equilibrium relation (2.9).

Define the following geometric quantities

$$A_x = \text{measure}(\Omega_x) = \int_{\Omega_x} d\Omega_x, \quad (4.1)$$

and

$$l_x = \text{measure}(\Gamma_x) = \int_{\Omega_x} \delta_{\Gamma_x} d\Omega_x = \int_{\Gamma_x} d\Gamma_x. \quad (4.2)$$

With this notation in hand, we introduce the weak equation

$$\boxed{-\frac{1}{A_x} \int_{\Omega_x} \boldsymbol{\gamma} \cdot \boldsymbol{\sigma} \mathbf{n} d\Omega_x + \frac{1}{l_x} \int_{\Gamma_x} \boldsymbol{\gamma} \cdot \mathbf{T} d\Gamma_x = 0 \quad \forall \boldsymbol{\gamma} \in \mathcal{J},} \quad (4.3)$$

imposed locally in  $\Omega_x$ . Note that the consideration of a material surface  $\Gamma_x$ , assumed massless in addition, results in no transient terms in (4.3).

A simple argument based on Taylor's expansion shows formally that equation (4.3) recovers the local equilibrium equation (2.9). To this purpose, define the length parameter

$$h_x := \frac{A_x}{l_x}. \quad (4.4)$$

The case of interest corresponds to the limit  $h_x \rightarrow 0$ , with  $A_x = O(h_x^{n_{\text{dim}}})$  and  $l_x = O(h_x^{(n_{\text{dim}}-1)})$ , so the neighborhood  $\Omega_x$  reduces to the point  $\mathbf{x}$  in the limit. The length scale  $h_x$  is chosen as the controlling parameter in this limit process. In this context, we consider the expansions

$$\boldsymbol{\sigma}(\mathbf{y}) = \boldsymbol{\sigma}_x + O(h_x), \quad \boldsymbol{\gamma}(\mathbf{y}) = \boldsymbol{\gamma}_x + O(h_x) \quad \forall \mathbf{y} \in \Omega_x, \quad (4.5)$$

and

$$\mathbf{T}(\mathbf{y}) = \mathbf{T}_x + O(h_x) \quad \forall \mathbf{y} \in \Gamma_x, \quad (4.6)$$

where  $(\cdot)_x = (\cdot)(\mathbf{x})$ , that is, the value of the corresponding quantity at the fixed point  $\mathbf{x} \in \Omega$ . The standard notation for the "big oh"  $O(\cdot)$ , that is,

$$\lim_{h_x \rightarrow 0} \frac{O(h_x^k)}{h_x^k} < \infty, \quad (4.7)$$

is considered in (4.7) and (4.6). Introducing the expansions (4.7) into (4.6), we obtain

$$[-\boldsymbol{\sigma}_x \mathbf{n} + \mathbf{T}_x] \cdot \boldsymbol{\gamma}_x + O(h_x) = 0 \quad \forall \boldsymbol{\gamma} \in \mathcal{J}, \quad (4.8)$$

so we recover formally the local equilibrium equation (2.9) in the local limit as  $h_x \rightarrow 0$ . We note that the Taylor's expansions considered in (4.7) and (4.6) involve regular fields. In particular, we consider the (smooth) displacement jumps and not the singular strains.

This situation is to be contrasted with the typical argument that relates traditional non-local models with higher-order models in terms of a Taylor's expansion of the total strain field, which becomes singular (unbounded), making the expansion argument questionable. See PIJAUDIER-CABOT et al [1995] for a discussion of these issues.

#### Remarks 4.1.

1. As presented in ARMERO [1997], an alternative argument shows that the relation (4.3) can be understood as the limit  $h_x \rightarrow 0$  of the imposed orthogonality condition

$$\int_{\Omega_x} \boldsymbol{\sigma} : \boldsymbol{\varepsilon}_{unres}^* d\Omega_x = 0, \quad (4.9)$$

between the stresses and the unresolved strain variations  $\boldsymbol{\varepsilon}^*$  defined as

$$\boldsymbol{\varepsilon}_{unres}^* = -\frac{1}{h_x} (\boldsymbol{\gamma} \otimes \mathbf{n})^s + (\boldsymbol{\gamma} \otimes \mathbf{n})^s \delta_{\Gamma_x} + O(1), \quad (4.10)$$

for variations  $\boldsymbol{\gamma} \in \mathcal{J}$ . The inclusion of (4.10) in (4.9) and the use of the relation (3.18) leads to the weak equation (4.3) in the case of interest  $h_x \rightarrow 0$ . The relation (4.9) imposes physically the vanishing of the stress power on the variations (4.10). Given (3.11), indicating that the large and small-scale strains ( $\boldsymbol{\varepsilon}(\mathbf{u})$  and  $\boldsymbol{\varepsilon}_\mu$ ) differ by the unresolved strains  $\boldsymbol{\varepsilon}_{unres}$ , the condition (4.9) equates the dissipation  $\mathcal{D}_\mu$  defined by (3.14) in the small scale to the dissipation observed in the local neighborhood  $\Omega_x$  by the large-scale problem involving the large-scale strains  $\boldsymbol{\varepsilon}(\mathbf{u})$ . Hence, the formulation developed above effectively incorporates then the localized dissipation of the small-scale response of the material in the (smooth) large-scale problem.

2. Furthermore, by understanding the unresolved strains as an enhancement of the large-scale strains  $\boldsymbol{\varepsilon}(\mathbf{u})$ , the orthogonality relation (4.9) falls within the class of enhanced strain methods as described in SIMO & RIFAI [1990]. It is important to note, however, that in this case the enhanced strains do not vanish in the limit  $h_x \rightarrow 0$ , but resolve the contributions of the localized strains associated to the strong discontinuity.  $\square$

#### 4.2. Large-scale regularization of rate-dependent models

The formulation presented in the previous section leads to a local continuum formulation in the limit  $h_x \rightarrow 0$ , incorporating the localized dissipation associated to the localized dissipative mechanism characterized in Section 3 by a strong discontinuity. As noted in Remark 4.1.1, the small-scale dissipation  $\mathcal{D}_\mu$  given by (3.14) is incorporated in the large-scale problem (2.5) by construction. Given the localized evolution equations (3.30), the localized part  $\tilde{\mathcal{D}}_\mu$  of the small-scale dissipation can be expressed as

$$\tilde{\mathcal{D}}_\mu = \tilde{\gamma} \tau_y \quad \text{on} \quad \Gamma_x, \quad (4.11)$$

as a simple calculation shows. The Perzyna viscoplastic regularization defined by (3.31) leads then to

$$\bar{D}_\mu = \frac{\langle g(\bar{\phi}) \rangle}{\eta_L} \tau_y \quad \text{on } \Gamma_x. \quad (4.12)$$

Therefore, for a finite value of the localized viscous parameter  $\eta_L$  we obtain a finite contribution to the final dissipation along the strong discontinuity  $\Gamma_x$ , even in the local continuum limit  $h_x \rightarrow 0$  (or, equivalently,  $1/h_x \rightarrow \infty$  emphasizing the idea of the large-scale limit).

As noted in the introduction, classical rate-dependent model with strain-softening incorporating a (continuum) viscosity are known to result in well-posed problems, still exhibiting the phenomena of strain localization and corresponding localized dissipation but now in a band of finite width  $w_s$ . Therefore, the consideration of a strong discontinuity and the corresponding finite dissipation on it does not comply with this observation. However, in the large-scale limit (that is, when  $h_x \gg w_s$ ), the above developments prove to be very useful for the actual numerical modeling of the localized dissipation observed in the small scale of the material. We note that in typical large-scale structural applications  $w_s \gg L$ , for a characteristic length scale  $L$  of the solid. The constructive procedure developed above (that is, the development of the constitutive relations in a finite neighborhood, and its actual incorporation in the large-scale problems) leads naturally to the finite element implementation of these ideas. As discussed in Section 4.3, this implementation is based on the identification of the local neighborhood  $\Omega_x$  with a finite element  $\Omega_e$ . The case  $h_x \gg w_s$  is then of the main interest, since it allows capturing the localized dissipation without the actual resolution of the small-scale length scales of order  $w_s$ . Still, the bulk dissipation needs to be recovered as  $h_x$  becomes of the order of the length scale  $w_s$ . This limit can be easily obtained by the proper scaling of the localized softening along  $\Gamma_x$  as developed next.

Given these considerations, we impose the condition

$$\bar{D}_\mu \sim \begin{cases} O(h_x) & \text{for } h_x/w_s \rightarrow 0, \\ O(1) & \text{for } h_x/w_s \gg 1, \end{cases} \quad (4.13)$$

for some estimate  $w_s$  of the width of the shear band. Given (4.12), this requirement is easily accomplished by defining the localized viscous parameter  $\eta_L$  through the scaling law

$$\eta_L^{-1} = \eta^{-1} l \quad \text{where } l = \min\{h_x, w_s\}, \quad (4.14)$$

for some finite viscous parameter  $\eta$  (units of stress/time). With this scaling and using (3.30)<sub>3</sub> and (3.31), we conclude that

$$\dot{\bar{\alpha}} = \dot{\bar{\gamma}} = \frac{\langle g(\bar{\phi}) \rangle}{\eta_L} \sim O(h_x) \quad \text{as } h_x \rightarrow 0. \quad (4.15)$$



Therefore, the localized softening modulus  $\mathcal{H}_L$ , defined by

$$\mathcal{H}_L = \widehat{\mathcal{H}}_L(\bar{\alpha}) := -\frac{dq(\bar{\alpha})}{d\bar{\alpha}}, \quad (4.16)$$

is of the order

$$\mathcal{H}_L \sim \tau_y \cdot O(h_x^{-1}) \quad \text{as } h_x \rightarrow 0, \quad (4.17)$$

after normalizing with  $\tau_y$  (units of stress) given (3.36). The scaling (4.17) is obtained by considering in this viscous case

$$\mathcal{H}_L^{-1} = \mathcal{H}^{-1} l, \quad (4.18)$$

for a softening modulus  $\mathcal{H}$  (units of stress), and  $l$  defined in (4.14)<sub>2</sub>. The reader is referred to Section 6 for several numerical examples illustrating these ideas.

### 4.3. The finite element implementation

The numerical implementation of the ideas developed in the previous sections follows along the lines of the finite element methods proposed in ARMERO & GARIKIPATI [1995,96], without the need of any regularization (smoothing) of the strong discontinuities. We summarize in this section the main ideas behind these methods and refer to these last references for further details.

The finite element implementation of the formulation developed above follows naturally by identifying the local neighborhood  $\Omega_x$  with a finite element  $\Omega_e$  of the assumed spatial discretization. We consider a piecewise constant approximation of the displacement jumps

$$\mathcal{J}^h = \{\xi_e \in \mathbb{R}^{n_{\text{dim}}} \text{ in } \Omega_e\}, \quad (4.19)$$

for each element  $\Omega_e$  where localization has been detected, admitting a straight discontinuity surface  $\Gamma_e$ . Higher order interpolations can be accommodated.

The interpolated total strain  $\boldsymbol{\varepsilon}_\mu^h$  is then given by

$$\boldsymbol{\varepsilon}_\mu^h = \boldsymbol{\varepsilon}(\mathbf{u}^h) + \boldsymbol{\varepsilon}_{\text{unres}}^h, \quad (4.20)$$

with the unresolved strain is given by (3.13) as

$$\boldsymbol{\varepsilon}_{\text{unres}}^h = -\frac{1}{h^{(i)}} \left( \xi_e^h \otimes \mathbf{n}^{(i)} \right)^s + \left( \xi_e^h \otimes \mathbf{n} \right)^s \delta_{\Gamma_e}, \quad (4.21)$$

the gradient of the discontinuous interpolation function

$$\boldsymbol{\varepsilon}_{\text{unres}}^h = \nabla^s \left[ (H_{\Gamma_e} + N_{\Gamma_e}^h) \xi_e^h \right] \quad \text{with} \quad N_{\Gamma_e}^h = 1 - \frac{(\mathbf{x} - \mathbf{x}^{(i)}) \cdot \mathbf{n}^{(i)}}{h^{(i)}}, \quad (4.22)$$

as depicted in Figure 4.1. See this figure for the notation employed in (4.21) and (4.22).

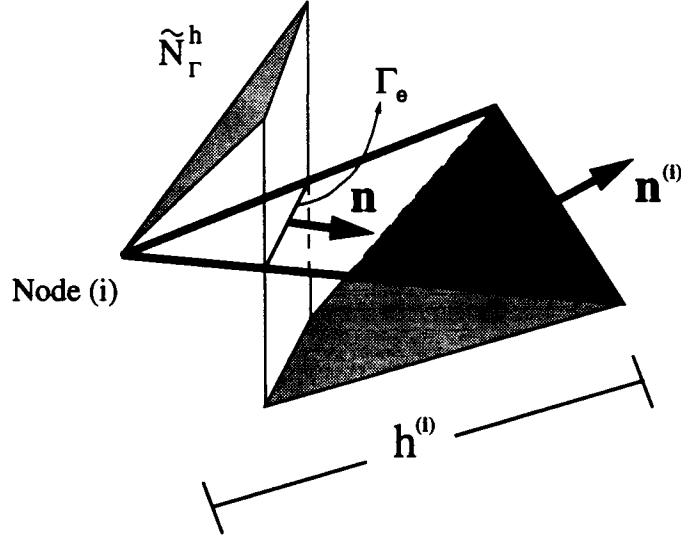


**FIGURE 4.1.** Discontinuous interpolation function motivating the choice of enhanced strain field.

In (4.20), the discretized large-scale strains are defined as

$$\boldsymbol{\varepsilon}(\mathbf{u}^h) = \mathbf{B}\mathbf{d}, \quad (4.23)$$

in a typical finite element  $\Omega_e$ , where  $\mathbf{B}$  denotes the standard linearized strain operator given by a standard finite element interpolation. For example, it may arise from some isoparametric interpolation of the large-scale displacements

$$\mathbf{u}^h = \mathbf{N}^h\mathbf{d}, \quad (4.24)$$

for the corresponding nodal displacements  $\mathbf{d}$ , or more generally from an assumed or mixed interpolation of the strains. The simulations in Section 6 consider mixed quadratic triangles with linear (discontinuous) interpolations of the pressure. See Figure 6.4.b.

The finite element formulation is based on the discrete counterpart of the weak equation (2.5) and the local nonlinear equation (4.3), leading to the set of algebraic system of equations in the nodal displacements  $\mathbf{d}$  and the local parameters  $\boldsymbol{\xi}_e^h$ .

$$\left. \begin{aligned} \mathbf{R} &:= \mathbf{f}_{ext} - \mathbf{A} \int_{\Omega_e} \mathbf{B}^T \boldsymbol{\sigma}(\mathbf{d}, \boldsymbol{\xi}_e^h) d\Omega - \mathbf{M}\ddot{\mathbf{d}} = 0 \\ \mathbf{s}_e &:= \frac{1}{A_e} \int_{\Omega_e} \boldsymbol{\sigma}(\mathbf{d}, \boldsymbol{\xi}_e^h) \mathbf{n} d\Omega - \mathbf{T}(\boldsymbol{\xi}_e^h) = 0 \quad \text{in } \Omega_e \end{aligned} \right\}, \quad (4.25)$$

where  $A_e = \text{measure}(\Omega_e)$ ,  $\mathbf{A}_{e=1}^{n_{elem}}$  refers to the standard assembly operator over the  $n_{elem}$  elements, and  $\mathbf{M}$  denotes the finite element mass matrix. We note the independence of

these parameters from element to element, consistent with the local character of the decomposition (3.1). As a practical consequence, this fact allows the efficient implementation of the proposed formulation through the static condensation of the local parameters  $\xi_e^h$ , leading to a final system of equations in the large-scale nodal displacements  $\mathbf{d}$ , after the consistent linearization of the equations. The resulting large-scale formulation incorporates the localized dissipation, as it was the original goal of the proposed approach.

## 5. The Extension to the Finite Deformation Range

We extend in this section the previous developments to the finite strain range. To this purpose, we summarize in Section 5.1 the finite kinematics of strong discontinuities, and develop in Section 5.2 the constitutive relations of localized dissipative mechanisms in the finite deformation range. Finally, Section 5.3 summarizes the finite element implementation in this geometrically nonlinear range.

### 5.1. The finite kinematics of strong discontinuities

The finite deformation of a solid occupying the reference placement  $\Omega \subset \mathbb{R}^{n_{\text{dim}}}$  is characterized in the large scale by the *smooth deformation* mapping  $\varphi : \Omega \rightarrow \mathbb{R}^{n_{\text{dim}}}$ . As it is customary, we denote the material points  $\mathbf{X} \in \Omega$  with the corresponding current position vectors as  $\mathbf{x} = \varphi(\mathbf{X})$ .

As in the infinitesimal case discussed in Section 3.3.1, the response of the material in a local neighborhood  $\Omega_X \subset \Omega$  of a material point  $\mathbf{X}$  may not be characterized completely by a smooth deformation field  $\varphi$ . We consider the case of a strong discontinuity given by the decomposition

$$\varphi_\mu = \varphi + \xi M_{\Gamma_x} \quad \text{in } \Omega_X, \quad (5.1)$$

with the function  $M_{\Gamma_x}$  defined as in (3.1), so  $\xi = [[\varphi_\mu]]$  across  $\Gamma_X \subset \Omega_X$ , a discontinuity surface with unit normal  $\mathbf{N}$  (a material vector). Considering the gradient of  $\varphi_\mu$  in  $\Omega_X$ , we obtain the expression

$$\mathbf{F}_\mu = \text{Grad}\varphi + \underbrace{\mathbf{G}_F(\xi) + \xi \otimes \mathbf{N} \delta_{\Gamma_X}}_{\mathbf{F}_{unres}}, \quad (5.2)$$

for the small-scale deformation gradient  $\mathbf{F}_\mu$ , with a regular part given by

$$\bar{\mathbf{F}}_\mu = \text{Grad}\varphi + \mathbf{G}_F(\xi). \quad (5.3)$$

The symbol  $\text{Grad}(\cdot)$  denotes the material gradient, with respect to the material coordinates  $\mathbf{X}$ . The regular part of the unresolved deformation gradient  $\mathbf{F}_{unres}$  is given by

$$\mathbf{G}_F(\xi) := \xi \otimes \text{Grad}N_{\Gamma_x} + \text{Grad}\xi H_{\Gamma_x} \quad \text{in } \Omega_x, \quad (5.4)$$

the counterpart of (3.8).

The expression (5.2) can be written alternatively as

$$\mathbf{F}_\mu = \bar{\mathbf{F}}_\mu (\mathbf{1} + \mathbf{J} \otimes \mathbf{N}), \quad (5.5)$$

for the material displacement jump vector

$$\mathbf{J} := \bar{\mathbf{F}}_\mu^{-1} [\boldsymbol{\varphi}_\mu]. \quad (5.6)$$

We decompose this material displacement jump in a material coordinate system

$$\mathbf{J} = \xi^i \mathbf{M}_i \quad (\text{summation implied}), \quad (5.7)$$

with  $\mathbf{M}_1 = \mathbf{N}$  and  $\mathbf{M}_i \cdot \mathbf{M}_j = \delta_{ij}$  (orthonormal), defining the convected coordinates  $\xi^i$ . We observe that the spatial displacement jump is given then as

$$[\boldsymbol{\varphi}_\mu] = \boldsymbol{\xi} = \xi^i \mathbf{m}_i^\sharp \quad \text{with} \quad \mathbf{m}_i^\sharp := \bar{\mathbf{F}}_\mu \mathbf{M}_i, \quad (5.8)$$

in the spatial configuration.

The nominal traction  $\mathbf{T}$  is introduced in this geometrically nonlinear setting as in (3.18) by the relation

$$\int_{\Omega_x} \mathbf{P} : (\boldsymbol{\gamma} \otimes \mathbf{N}) \delta_{\Gamma_x} d\Omega_x = \int_{\Gamma_x} \mathbf{T} \cdot \boldsymbol{\gamma} d\Gamma_x \quad \forall \boldsymbol{\gamma} \in \mathcal{J}, \quad (5.9)$$

in terms of the nominal stresses  $\mathbf{P}$  (first Piola-Kirchhoff stress tensor). Similarly, we define the covariant components of the traction as

$$\mathbf{T} = T_i \mathbf{m}_\beta^i \quad \text{with} \quad \mathbf{m}_\beta^i = \bar{\mathbf{F}}_\mu^{-T} \mathbf{M}_i, \quad (5.10)$$

We note the orthogonality relations  $\mathbf{m}_j^\sharp \cdot \mathbf{m}_\beta^i = \delta_j^i$  (the Kronecker delta). In particular, we define the spatial normal vector

$$\mathbf{n}_\beta \equiv \mathbf{m}_\beta^1 = \bar{\mathbf{F}}_\mu^{-T} \mathbf{N}, \quad (5.11)$$

not a unit vector, in general.

As shown in ARMERO & GARIKIPATI [1996], the response of the strong discontinuities in finite strain models of multiplicative plasticity can be characterized by the Lie derivative of the displacement jumps defined as

$$\boldsymbol{\mathcal{L}}_{\mathbf{v}} [\boldsymbol{\varphi}_\mu] := \bar{\mathbf{F}}_\mu \frac{d}{dt} [\bar{\mathbf{F}}_\mu^{-1} [\boldsymbol{\varphi}]] = \bar{\mathbf{F}}_\mu \mathbf{j}. \quad (5.12)$$

The vector  $\mathbf{L}_v[\varphi_\mu]$  defines a frame-indifferent (objective) rate of the change of the displacement jump  $[\varphi_\mu]$ . Furthermore, combining (5.12) with (5.8) we obtain

$$\mathbf{L}_v[\varphi_\mu] = \dot{\xi}^i \mathbf{m}_i^\#, \quad (5.13)$$

in the coordinate system defined in (5.8)<sub>2</sub>.

## 5.2. Localized dissipative mechanisms in the finite deformation range

Motivated by the results in the infinitesimal case, we consider similarly a decomposition of the stored energy of the material in a continuum and localized contributions

$$W(\mathbf{F}_\mu, \mathcal{I}) = \bar{W}(\bar{\mathbf{F}}_\mu^T \bar{\mathbf{F}}_\mu, \bar{\mathcal{I}}) + \tilde{W}(\mathbf{J}, \tilde{\mathcal{I}}) \delta_{\Gamma_X}, \quad (5.14)$$

where the dependence on the right Cauchy-Green tensor  $\bar{\mathbf{F}}_\mu^T \bar{\mathbf{F}}_\mu$  for the continuum contribution and  $\mathbf{J}$  (or alternatively, the components  $\xi^i$ ) for the localized part is imposed in accordance with the *principle of material frame indifference*, as a classical argument shows. The regular part  $\bar{W}$  of the stored energy function leads to standard continuum models in  $\Omega_X/\Gamma_X$  for, say, the nominal stresses  $\mathbf{P}$  (first Piola-Kirchhoff stress tensor). Furthermore, we define the *frame-indifferent measure*

$$\tilde{\mathcal{D}}_\mu := T_i \dot{\xi}^i - \dot{\tilde{W}}, \quad (5.15)$$

along the discontinuity  $\Gamma_X$  to base the arguments of the derivation of the localized constitutive relations. Equation (5.15) has the same form as its infinitesimal counterpart (3.17) in the considered convected basis.

The formulation of a localized elastoplastic model follows then by considering the elastoplastic decomposition

$$\boxed{\mathbf{J} = \mathbf{J}^e + \mathbf{J}^p}, \quad (5.16)$$

in a elastic and a plastic part. We note that the spatial decomposition

$$\boldsymbol{\xi} = \boldsymbol{\xi}^e + \boldsymbol{\xi}^p, \quad (5.17)$$

follows with the definitions

$$\boldsymbol{\xi}^e := \bar{\mathbf{F}}_\mu \mathbf{J}^e \quad \text{and} \quad \boldsymbol{\xi}^p := \bar{\mathbf{F}}_\mu \mathbf{J}^p, \quad (5.18)$$

with  $\boldsymbol{\xi} = \bar{\mathbf{F}}_\mu \mathbf{J}$  by (5.3). The corresponding expressions in the considered convected basis read

$$\mathbf{J}^e = \xi^{ei} \mathbf{M}_i \quad \text{and} \quad \mathbf{J}^p = \xi^{pi} \mathbf{M}_i, \quad (5.19)$$

with the elastoplastic decomposition

$$\xi^i = \xi^{ei} + \xi^{pi} \quad (i = 1, n_{\text{dim}}), \quad (5.20)$$

of the convected components of the displacement jumps follows.

The same arguments employed in the infinitesimal case lead then to the constitutive relation

$$T_i = \frac{\partial \bar{W}}{\partial \xi^{e^i}} \quad (i = 1, n_{\text{dim}}), \quad (5.21)$$

for the nominal tractions, and

$$\bar{D}_\mu = T_i \dot{\xi}^{p^i} + q \dot{\bar{\alpha}}, \quad (5.22)$$

for the localized measure, with stress-like internal variable  $q$  defined again by (3.25). The maximization of (5.22) among all admissible stress states  $\bar{\phi}(\mathbf{T}, q) \leq 0$ , as done in Section 3 for the infinitesimal case, leads to the associated plastic evolution equations

$$\left. \begin{aligned} \dot{\xi}^{p^i} &= \bar{\gamma} \frac{\partial \bar{\phi}}{\partial T_i} \quad (i = 1, n_{\text{dim}}), \\ \dot{\bar{\alpha}} &= \bar{\gamma} \frac{\partial \bar{\phi}}{\partial q}, \end{aligned} \right\} \quad (5.23)$$

together with the Kuhn-Tucker loading/unloading conditions

$$\bar{\phi} \leq 0, \quad \bar{\gamma} \geq 0, \quad \text{and} \quad \bar{\gamma} \bar{\phi} = 0, \quad (5.24)$$

and the consistency condition

$$\bar{\gamma} \dot{\bar{\phi}} = 0, \quad (5.25)$$

as their infinitesimal counterparts. The Perzyna viscoplastic regularization is given by

$$\bar{\gamma} = \frac{\langle g(\bar{\phi}) \rangle}{\eta_L}, \quad (5.26)$$

as developed in Section 3.

A rigid (visco)plastic slip model is obtained in the same way as discussed in Section 3.3.1 for the infinitesimal case. The slip surface (3.35) is considered again with the norm of the tangential traction vector defined by

$$\mathbf{T}_T = \sum_{\beta=2}^{n_{\text{dim}}} T_\beta \mathbf{M}^\beta \quad \text{and} \quad \|\mathbf{T}_T\|^2 = \sum_{\alpha, \gamma=2}^{n_{\text{dim}}} T_\alpha \delta^{\alpha\beta} T_\beta, \quad (5.27)$$

for the dual basis  $\mathbf{M}^i \equiv \mathbf{M}_i$  given the orthonormal character assumed for the material basis  $\{\mathbf{M}_i\}$ . The rigid plastic slip equations (3.37) hold then in this case

$$\left. \begin{aligned} \delta_{\beta\alpha} \dot{\xi}^\alpha &= \bar{\gamma} \frac{T_\beta}{\|\mathbf{T}_T\|} \quad (\beta = 2, n_{\text{dim}}), \\ \dot{\xi}^1 &= 0, \\ \dot{\bar{\alpha}} &= \bar{\gamma}, \end{aligned} \right\} \quad (5.28)$$



with  $\xi^e \equiv 0$ , as a simple calculation shows.

**Remark 5.1.** The above formulation corresponds to a fully material characterization of a localized dissipative mechanism on  $\Gamma_x$ . As shown above, it leads to governing equations possessing the same form as their infinitesimal counterparts. Alternative formulations that, for example, do not consider a fixed (orthonormal) material basis  $\{\mathbf{M}_i\}$ , with the slip yield condition defined in terms of a spatial norm of the tangential traction vector (involving spatial, true stress components) can also be developed. Details are omitted. This situation is similar to the modeling of frictional contact of solids, as discussed in LAURSEN [1994].  $\square$

### 5.3. The governing equations and their finite element implementation

The counterpart of the the large-scale problem (2.5) in the finite deformation considered in this section can be similarly expressed in terms of the unknown (smooth) deformation  $\varphi \in \mathcal{V} + \bar{g}$ ,

$$\int_{\Omega} \rho_o \ddot{\varphi} \cdot \eta \, d\Omega + \int_{\Omega} \mathbf{P} : \text{Grad} \eta \, d\Omega = \int_{\Omega} \rho_o \mathbf{b} \cdot \eta \, d\Omega + \int_{\partial_{\tau} \Omega} \bar{\mathbf{t}} \cdot \eta \, d\Gamma \quad \forall \eta \in \mathcal{V}, \quad (5.29)$$

for given initial conditions  $\varphi(\mathbf{x}, 0) = \varphi_o(\mathbf{x})$  and  $\dot{\varphi}(\mathbf{x}, 0) = \mathbf{v}_o(\mathbf{x})$ , with the nominal stresses  $\mathbf{P}$  given by the constitutive relations as described in the previous section. Equivalently, the internal virtual work term can be written as

$$\int_{\Omega} \mathbf{P} : \text{Grad} \eta \, d\Omega = \int_{\Omega} \boldsymbol{\tau} : \nabla^s \eta \, d\Omega, \quad (5.30)$$

in terms of the Kirchhoff stress field  $\boldsymbol{\tau}$  defined as

$$\boldsymbol{\tau} = \mathbf{P} \bar{\mathbf{F}}_{\mu}^T, \quad (5.31)$$

and the spatial gradient defined by

$$\nabla \eta := \bar{\mathbf{F}}_{\mu}^{-T} \text{Grad} \eta, \quad (5.32)$$

both using the regular part of the deformation gradient  $\bar{\mathbf{F}}_{\mu}$ .

The localized constitutive model developed in the previous section is incorporated in the large-scale problem (5.29) as in the infinitesimal case by considering the weak form of the local equilibrium equation across the *material* surface  $\Gamma_X$

$$-\frac{1}{A_X} \int_{\Omega_X} \boldsymbol{\gamma} \cdot \boldsymbol{\tau} \mathbf{n}_{\beta} \, d\Omega_x + \frac{1}{l_X} \int_{\Gamma_X} \boldsymbol{\gamma} \cdot \mathbf{T} \, d\Gamma_x = 0 \quad \forall \boldsymbol{\gamma} \in \mathcal{J}, \quad (5.33)$$

with  $\mathbf{n}_{\beta}$  given by (5.11), and  $A_X = \text{measure}(\Omega_X)$  and  $l_X = \text{measure}(\Gamma_X)$  defined as in (4.1) and (4.2), respectively.

The finite element implementation follows then as in the infinitesimal case, leading to the discrete equations

$$\left. \begin{aligned} \mathbf{R} &:= \mathbf{f}_{ext} - \mathbf{A} \int_{\Omega_e} \mathbf{b}^T \boldsymbol{\tau} d\Omega - \mathbf{M} \ddot{\mathbf{d}} = 0, \\ \mathbf{s}_e &:= \frac{1}{A_e} \int_{\Omega_e} \boldsymbol{\tau} \mathbf{n}_\beta d\Omega - \mathbf{T}(\boldsymbol{\xi}_e^h) = 0 \quad \text{in } \Omega_e, \end{aligned} \right\} \quad (5.34)$$

for a spatial linearized discrete strain operator  $\mathbf{b}$  and finite element  $\Omega_e$  in the reference configuration of the solid. The efficient numerical implementation of the equations (5.34) involves again the static condensation of the element parameters  $\boldsymbol{\xi}_e^h$  after their consistent linearization. Further details can be found in ARMERO & GARIKIPATI [1996], and are omitted here.

**Remark 5.2.** The general elastoplastic framework developed in Section 5.2 allows the elastic regularization of the rigid localized mechanism defined by (5.28). In this way, we consider the elastic relation

$$T_i = \kappa_i \xi^{ei} \quad i = 1, n_{\text{dim}} \quad (\text{no sum}), \quad (5.35)$$

for large (penalty) parameters  $\kappa_i$ . The final governing equations (5.23) possess then the same structure of (infinitesimal) elastoplasticity, allowing then the application of standard return mapping algorithms for their numerical integration. The reader is referred to SIMO & HUGHES [1997] for details. Implementations not involving the regularization (5.35) can be found in ARMERO & GARIKIPATI [1995].  $\square$

## 6. Representative Numerical Simulations

We present in this section the results obtained for two representative examples that assess the performance of the numerical modeling of viscoplastic strain localization through strong discontinuities as described in the previous sections. Section 6.1 includes the results obtained in the 1D wave propagation problem in an infinitesimal viscoplastic shear layer. The benchmark problem given by the simulation of the plane strain tension test at finite strains is discussed in Section 6.2.

### 6.1. 1D wave propagation problem in a softening viscoplastic shear layer

We consider the one-dimensional dynamic problem of the propagation of shear waves in a viscoplastic shear layer. Infinitesimal conditions are assumed. A layer width  $L = 100$  and unit thickness is considered, under simple shear conditions, with a fixed left end ( $v = 0$  at  $x = 0$  and all times) and an imposed sudden shear stress  $\tau_o$  at the right end  $x = L$ .

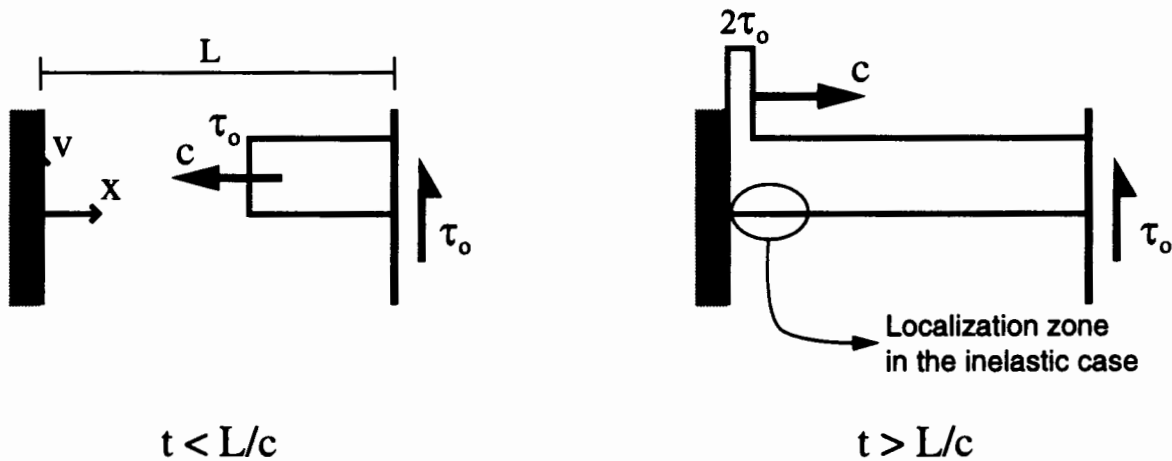


**FIGURE 6.1.** 1D wave propagation problem. Sketch of the elastic solution. After reflection at the fixed end the stress doubles in the elastic case. In the inelastic case, the material yields and softens creating a shear band.

Figure 6.1 depicts the definition of the problem, as well as the elastic solution. In this case, a pulse of constant stress  $\tau_0$  travels along the layer at a constant wave speed  $c = \sqrt{G/\rho}$ , for a shear modulus  $G$  and density  $\rho$ . Upon reaching the fixed end, the stress doubles in this elastic case, and is reflected back along the shear layer.

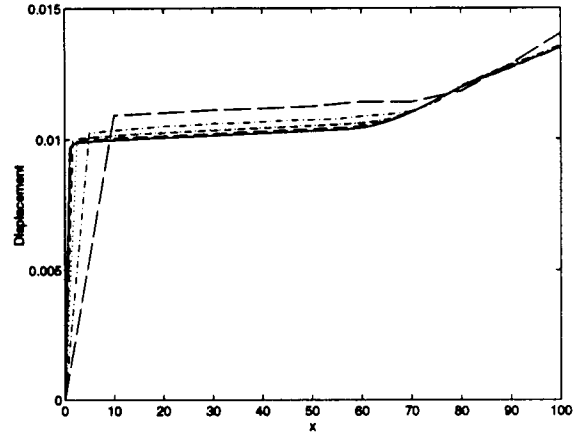
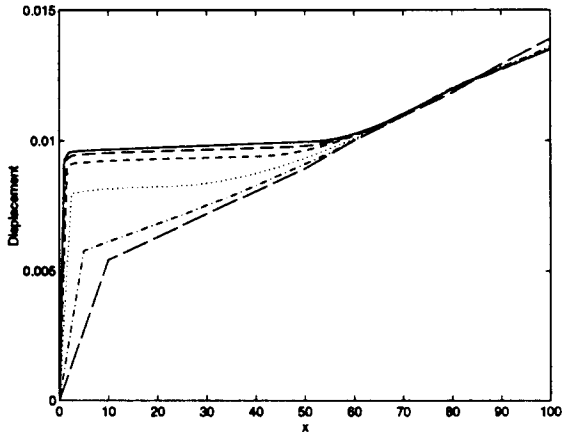
In the case of a softening material, a shear band appears at the fixed end upon reflection if the yield limit of the material is reached. The problem of a rate-independent softening material (in its completely equivalent form involving an axial bar) has been considered in BAZANT & BELYTSCHKO [1985]. In this case, the well-known pathological mesh-size dependence of the finite element solution appears as a consequence of the inability of a rate-independent material model involving a fixed softening strain/stress relation to capture the localized dissipative mechanism associated to the shear band. As noted in the introduction, these difficulties can be traced back to the absence of a material length scale in such a model. The results presented in NEEDLEMAN [1988] and SLUYS [1992] for this same problem show the regularizing effects of the inclusion of viscosity in the inelastic material law. A material length scale is introduced in the material model, leading to finite element solutions converging to a finite shear band width, and avoiding the pathological mesh-dependence *in the limit, as this material length scale is resolved by the mesh*. See the aforementioned references for details. However, we should expect a bad performance by meshes not resolving the very small scale associated to typical materials of interest.

Figure 6.2, left column, depicts the results obtained for the viscoplastic model characterized by the elastic relation  $\tau = G(\gamma - \gamma^p)$  in terms of the shear stress  $\tau$ , engineering shear strain  $\gamma = \partial v / \partial x$  and the plastic shear strain  $\gamma^p$ . The latter is defined by the viscoplastic

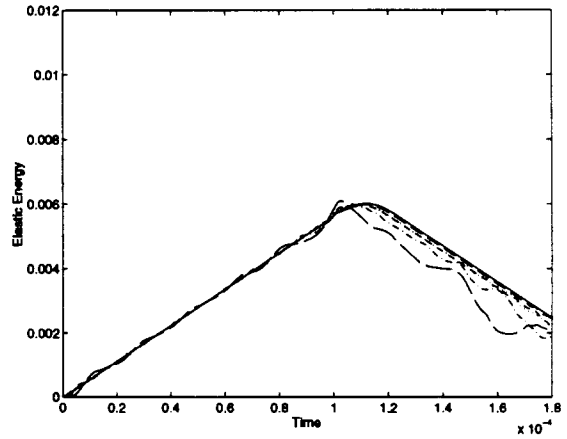
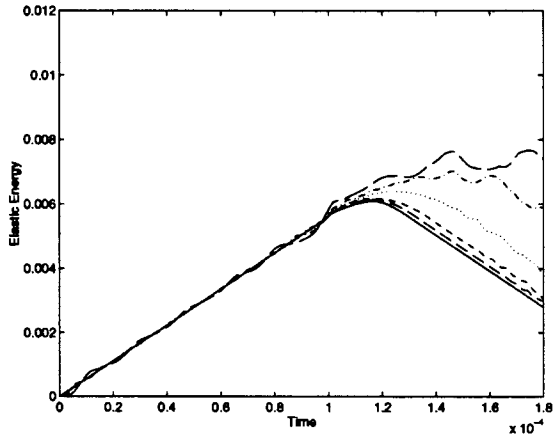
**SOFTENING VISCOPLASTICITY**

**LOCALIZED VISCOUS MODEL**

**Displacement**



**Elastic Energy**



**Dissipated Energy**

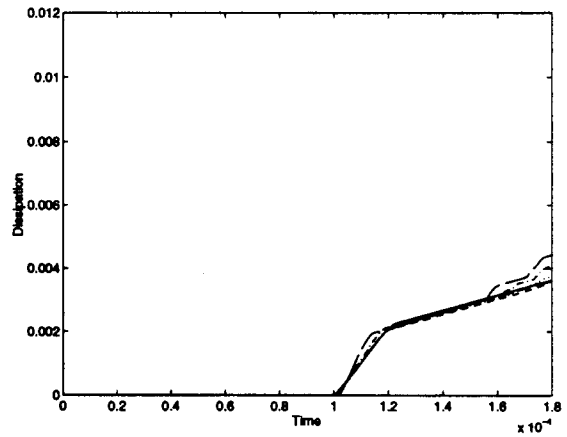
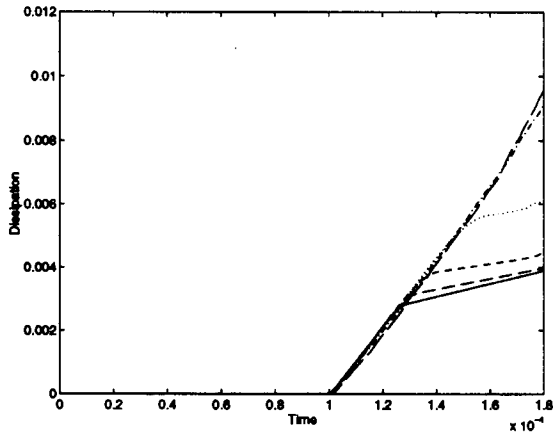


**FIGURE 6.2.** 1D wave propagation problem. Solutions obtained with a classical viscoplastic model with strain-softening and a localized viscous model for a viscosity  $\eta = 1 \cdot 10^{-3}$ . The mesh-dependence for the classical viscoplastic model for coarse meshes can be seen alleviated with the use of a localized dissipative mechanism. Legend: — (h = 10), - - - (h = 5), ····· (h = 2.5), - - - - (h = 1.67), - - - - (h = 1.25), — (h = 1).

**SOFTENING VISCOPLASTICITY**

**LOCALIZED VISCOUS MODEL**

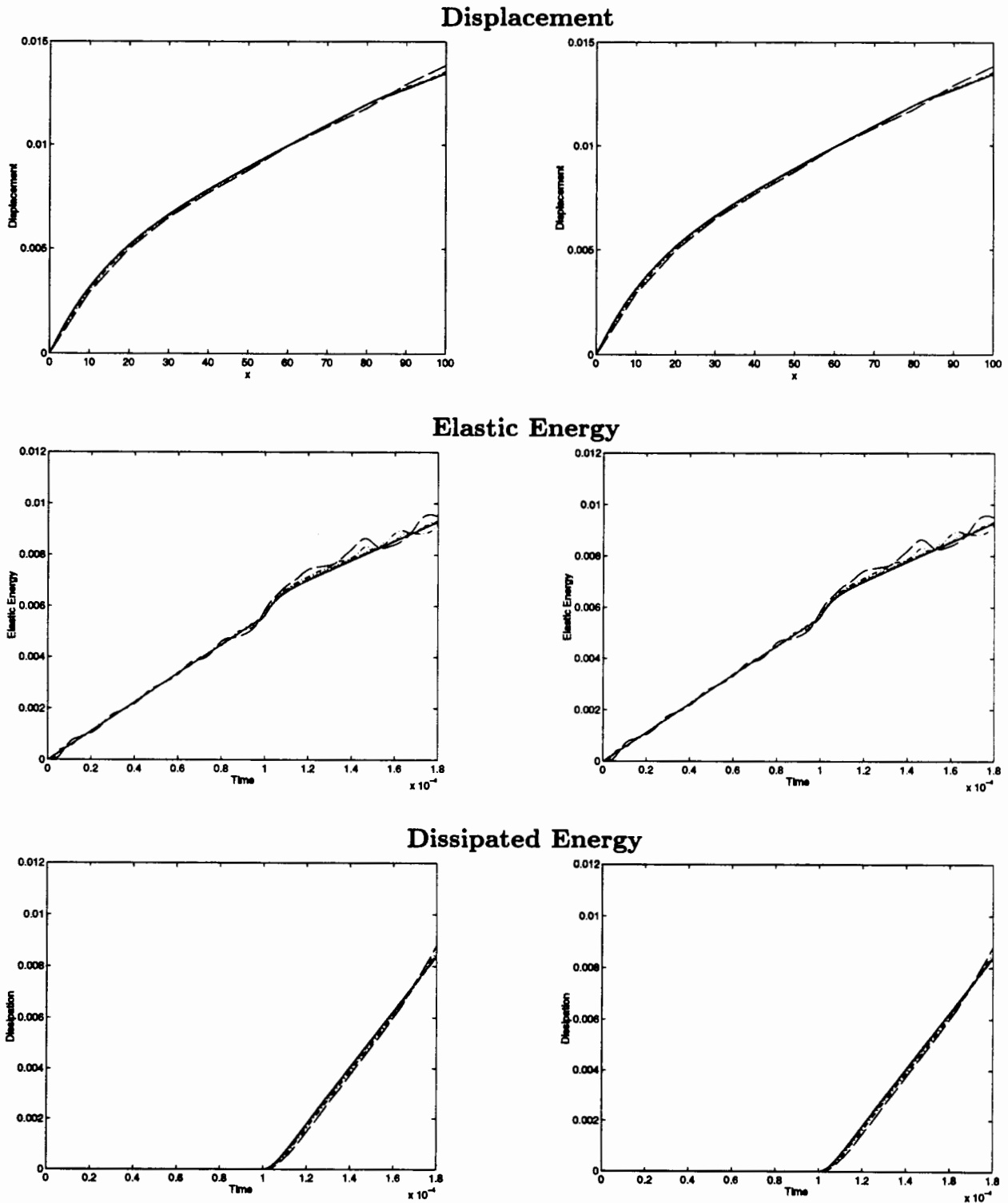


**FIGURE 6.3.** 1D wave propagation problem. Solutions obtained with a classical viscoplastic model with strain-softening and a localized viscous model for a viscosity  $\eta = 1 \cdot 10^{-1}$ . The same solution is obtained in both cases, exhibiting a very low mesh dependence in this case of high viscosity. Legend:  $-\cdot-\cdot-$  ( $h = 10$ ),  $- - -$  ( $h = 5$ ),  $\cdot\cdot\cdot\cdot\cdot$  ( $h = 2.5$ ),  $- \cdot - \cdot -$  ( $h = 1.67$ ),  $- - - \cdot - -$  ( $h = 1.25$ ),  $—$  ( $h = 1$ ).

evolution equations

$$\left. \begin{aligned} \dot{\gamma}^p &= \frac{\langle \phi \rangle}{\eta} \text{sign}(\tau) , \\ \dot{\alpha} &= \frac{\langle \phi \rangle}{\eta} , \\ \phi &= |\tau| - \max\{\tau_y + \mathcal{H}\alpha, 0\} . \end{aligned} \right\} \quad (6.1)$$

The following material properties are assumed: shear modulus  $G = 2 \cdot 10^4$ , initial yield limit  $\tau_y = 2$ , softening modulus  $\mathcal{H} = -1 \cdot 10^3$ , and viscosity parameter  $\eta = 1 \cdot 10^{-3}$ . The density of the material is  $\rho = 2 \cdot 10^{-8}$ , leading to an elastic wave speed of  $c = 2 \cdot 10^6$ . The initial sudden shear stress pulse applied to the layer is  $\tau_o = 0.75 \tau_y$ , leading to the yielding of the material upon the reflection of the wave. The dynamic governing equations are integrated through the trapezoidal rule with a consistent mass matrix. A time step of  $\Delta t = L/(200 c)$  is employed. The shear layer is discretized with different number of linear finite elements to study the effectiveness in resolving the localized shear band.

The top, left plot in Figure 6.2 shows the displacement distribution along the bar for this case of (continuum) softening viscoplasticity. We observe for the fine meshes the sharp gradient of this distribution at the left end  $x = 0$ , thus obtaining the expected formation of the shear band. We can observe the converging approximation as the finite element size  $h$  is reduced. But we can observe at the same time the bad resolution of the final localized solution for large mesh sizes, leading to a strong mesh dependence for the coarse meshes. This dependence is illustrated by the plots in Figure 6.2. We have included the evolution in time of the elastic energy in the shear layer

$$W_{elas} = \int_0^L \frac{1}{2} \frac{\tau^2}{G} dx , \quad (6.2)$$

and the total dissipated energy

$$\mathcal{D} = W_{ext} - W_{elas} - K , \quad (6.3)$$

for the applied external work (due to the applied stress at the right end)

$$W_{ext} = \int_0^t \tau_o v(L, t) dt , \quad (6.4)$$

and the kinetic energy

$$K = \int_0^L \frac{1}{2} \rho v^2 dx . \quad (6.5)$$

The strong dependence on the mesh-size if the localized zone is not resolved by the mesh is apparent.

To capture the localized dissipative mechanism associated to the shear band, we consider the localized viscous model developed in Section 3 instead of the continuum inelastic



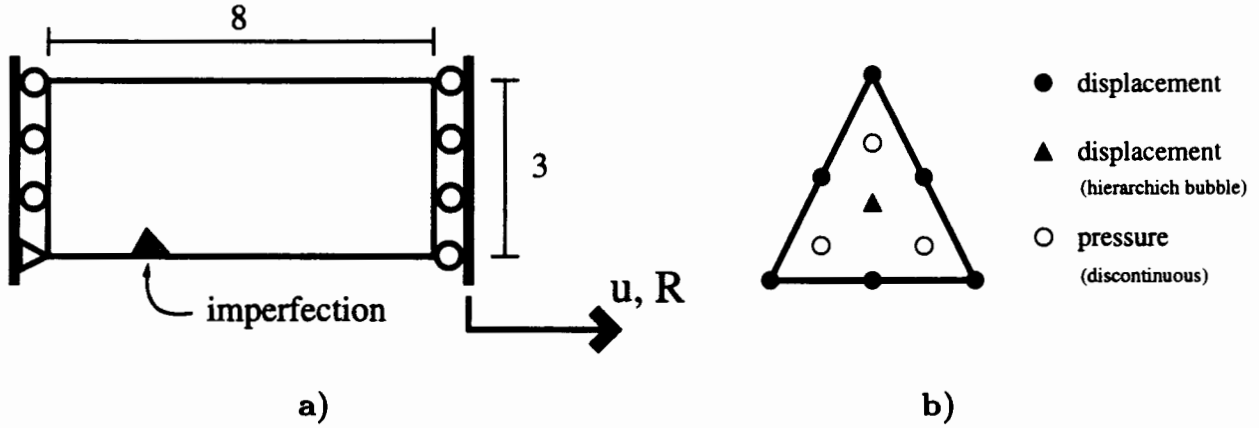


**FIGURE 6.4.** Plane strain tension test. **a)** Problem definition, with an imposed displacement  $\bar{u}$  at the right end and measured load  $R$ ; **b)**  $P2 \oplus$  bubble /  $P1$  element.

equations (6.1), maintaining the linear elastic relation for the continuum. This is done only in the first element of the fixed end, once yielding is detected. The rest of the shear layer remains viscoplastic. We note that in this simple one-dimensional example the loss of ellipticity of the underlying rate-independent softening model occurs at the initiation of yielding; see Remark 3.1. We note also that  $\mathbf{n} \equiv 1$  in this one-dimensional case.

The localized softening modulus  $\tilde{\eta}_L$  and  $\tilde{\mathcal{H}}_L$  are defined through the scaling relations (4.14) and (4.18), respectively. The parameter  $w_s$  in (4.14)<sub>2</sub> is chosen as the element size that resolves the shear band. We note that this parameter is to be understood a numerical parameter and *not a material property*. The relation (4.14)<sub>2</sub> effectively switches from the localized dissipated mechanism associated to the strong discontinuity to a continuum dissipative as the element size goes below  $w_s$ .

Figure 6.2, right column shows the result obtained with the localized viscous model. A value  $w_s = L/100$  is considered. We observe the completely different solutions for the coarse meshes, resolving more accurately the localized solution associated to the appearance of the shear band. Coarse meshes that were unable to give a accurate solutions for the continuum model lead in this case to meaningful displacement distributions. In particular, the numerical solutions are seen to capture more accurately the evolution of the dissipation in time.

Figure 6.3 shows the result obtained for a large viscosity  $\eta = 1 \cdot 10^{-1}$ . The solution in this case is essentially smooth, as shown in the displacement distribution. The localized viscous model is considered with  $w_s = L/2$ , leading for the assumed mesh sizes to a scaling parameter  $l = h$ . In this situation, the mesh resolves the details of the solution, leading both the continuum and the localized viscous models to the same solution in this 1D setting. A simple calculation shows that the localized viscous model (3.30) is obtained

TABLE 6.1. Plane strain tension test. Material properties.

|                               |                         |                   |
|-------------------------------|-------------------------|-------------------|
| Bulk Modulus                  | $\kappa$                | 164.206           |
| Shear Modulus                 | $\mu$                   | 80.1938           |
| Uniaxial Yield Limit          | $\sigma_y$              | 45.0              |
| Viscosity                     | $\eta$                  | $1 \cdot 10^{-3}$ |
| Localized softening modulus   | $\tilde{\mathcal{H}}_L$ | -12.0             |
| Localized viscosity parameter | $\tilde{\eta}_L$        | $1 \cdot 10^{-3}$ |

from the continuum model (6.1) with the identifications  $\gamma^p \leftarrow \xi/h$  (the regular part of the unresolved strains) and  $\alpha \leftarrow \tilde{\alpha}/h$  in this particular case ( $h < w_s$ ) of the one dimensional problem.

In conclusion, the proposed formulation, consisting basically of the appropriate scaling in this simple one dimensional setting, recovers the continuum solution as the spatial discretizations resolves the details of the localized solution, while leading to a more accurate resolution of the same in coarse meshes. The “large-scale regularization” of the localization of the strains in rate-dependent models is effectively obtained.

## 6.2. The plane strain tension test

We consider the plane strain tension test in this second example. Complete numerical analyses of this benchmark problem can be found in TVERGAARD et al. [1981] and references therein. Figure 6.4 depicts the problem under consideration. A  $8 \times 3$  block is stretched under an imposed displacement at one edge, while considering smooth boundary conditions at both ends. Quasi-static conditions are assumed in this case. The finite strain  $J_2$ -flow theory of viscoplasticity with the numerical implementation as discussed in SIMO [1992] is considered for the bulk response, in combination with the finite strain localized viscous model described in Section 5. The material properties are summarized in Table 6.2. In particular, perfect viscoplasticity is considered for the continuum model, and a linear localized softening law given by  $\tau_y = \sigma_y/\sqrt{3}$  and the localized softening modulus  $\tilde{\mathcal{H}}_L$ . See Table 6.2. Due to the symmetry in the problem a small imperfection (0.1% reduction of the uniaxial yield limit  $\sigma_y$ ) is considered in an element of the lower boundary. Different spatial discretizations, including structured and unstructured meshes, based on the  $P2 \oplus \text{bubble} / P1$  quadratic triangle depicted in Figure 6.4.b are considered. This element can be shown to pass the LBB condition in the incompressible infinitesimal case (as proposed in CROUZEIX & RAVIART [1973]), avoiding the volumetric locking common in elastoplastic calculations. We note in this respect, and as discussed below, the appearance of the localized solution is preceded by a certain amount of bulk plastic flow.

The localized inviscid solution for this problem was reported in ARMERO & GARIKIPATI

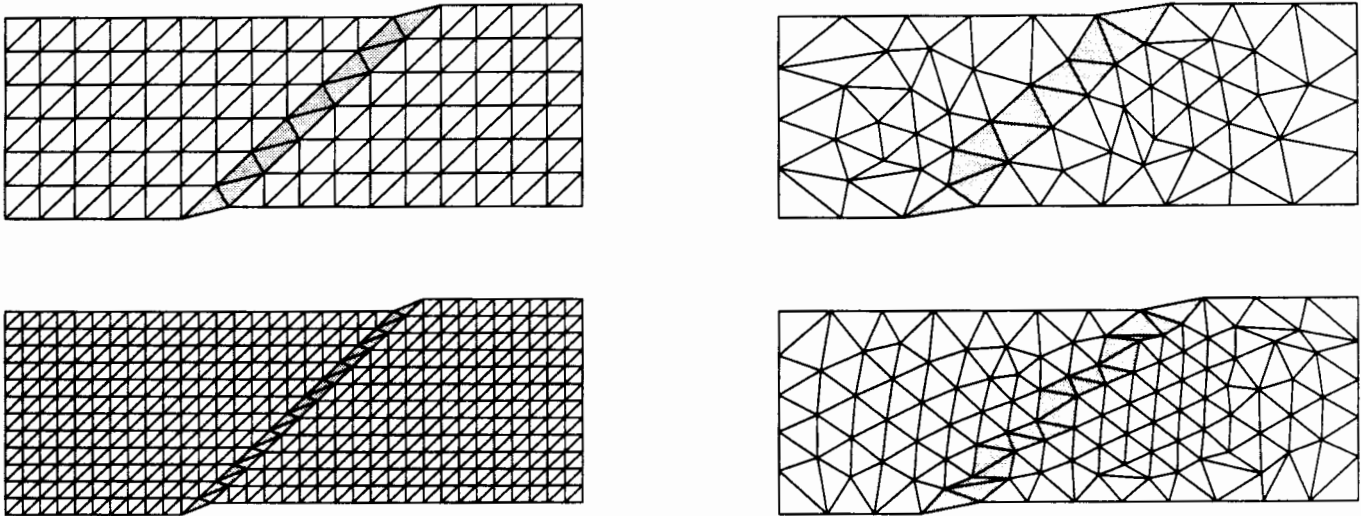


**FIGURE 6.5.** Plane Strain Tension test. Localized viscous model ( $\eta = 1 \cdot 10^{-3}$ ). Solutions computed with the  $P2 \oplus \text{Bub}/P1$  triangle and enhanced localization modes in structured (192 and 768 elements) and unstructured (102 and 199 elements) meshes (End displacement = 0.08, deformations scaled by 5).

[1996]. Figure 6.5 depicts the solution obtained in the case of a viscous discontinuity. The elements exhibiting active enhanced localization modes are shown in gray in Figure 6.5. A perfectly viscoplastic material is assumed until localization is detected, resulting then in the consideration of the enhanced modes modeling the strong discontinuity with the corresponding localized softening law. A linear softening law is assumed. Elements outside the path of the discontinuity remain viscoplastic. As discussed in Remark 3.1, the loss of ellipticity condition of the underlying rate-independent solid is considered to determine the orientation of the discontinuity. A closed-form expression for the current case of  $J_2$ -flow theory can be found in ARMERO & GARIKIPATI [1995]. We note that the discontinuity is propagated as the solution is computed, with no predetermined path. The reader is referred to these last references for details on these issues.

Figure 6.6 depicts the load/displacement curves obtained in this case. The rate-independent solution is also included. In both the viscid and inviscid problems the solutions for four different meshes are included. Structured and unstructured meshes, involving from 102 to 768 elements, are considered; see Figure 6.5. Almost a perfect overlapping of the curves can be observed. The low mesh sensitivity of the proposed methodology is apparent in this problem. We observe the stiffer response of the viscoplastic solution, with the appearance and propagation of the localized solution at a later deformation compared to the inviscid solution.

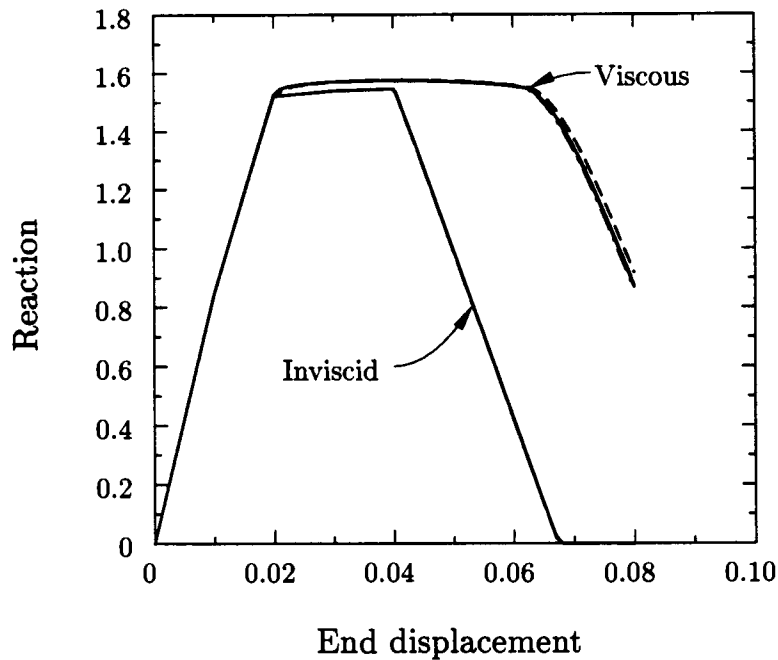


**FIGURE 6.6.** Plane Strain Tension test. Load/displacement curves for the localized viscous model and the inviscid limit model, computed with the  $P2 \oplus \text{Bub}/P1$  triangle and enhanced localization modes in structured and unstructured meshes. **Legend:** Coarse unstructured mesh, 102 elements (---); Fine unstructured mesh, 199 elements (- · -); Coarse structured mesh, 192 elements (- -); Fine structured mesh, 768 elements (—).

## 7. Conclusions

The modeling of localized dissipative mechanisms in a local continuum has been accomplished with the use of the formalism of strong discontinuities. The case of elastoplastic discontinuities, and their viscous regularization, has been considered in both the infinitesimal and finite deformation ranges. In both cases, localized constitutive models have been developed locally without the need of the introduction of (smearing) length scales. The inclusion of these models in the smooth problem governing the large-scale response of the solid identifies the length scales appearing in the modeling of localized solutions. The limit of interest as these scales vanish (the large-scale limit) identifies the structure of a local continuum incorporating the localized dissipation characteristic of the localized failure of common materials.

A first application of the previous developments is the formulation of sound constitutive models incorporating objectively a localized dissipation. Rate-independent continuum models are known for the absence of a characteristic length defining the small scales of

the final localized solutions, leading to the limit case of strong discontinuity. The proposed formulation identifies the localized dissipation characteristic of these solutions, thus leading to a large-scale model of the phenomenon of strain localization with the correct (objective) energy dissipation.

The large-scale regularization of rate-dependent models has been introduced as a second application of the proposed approach. In this viscous case, the continuum models are known to incorporate the length scales required to define the observed localized dissipation. The small scales involved in these solutions when compared with typical scales of the practical applications of interest lead to numerical solutions with a strong mesh-dependence, unless costly spatial discretizations resolving the small scales are considered. The proposed approach models effectively the unresolved scales through the consideration of strong discontinuities, the large-scale limit. Furthermore, the proper scaling of the associated localized mechanism allows the recovery of the proper dissipation as the small scales are resolved.

### Acknowledgments

Financial support for this research has been provided by the ONR under contract no. N00014-96-1-0818 with UC Berkeley. This support is gratefully acknowledged.

### References

- ARMERO, F. [1997] "Formulation and Numerical Analysis of a Localized Anisotropic Damage Model," SEMM/UCB Report no. 97/11, submitted for publication.
- ARMERO, F. & GARIKIPATI, K. [1995] "Recent Advances in the Analysis and Numerical Simulation of Strain Localization in Inelastic Solids," *Proc. COMPLAS IV*, eds. D.R.J. Owen, E. Onate, and E. Hinton, CIMNE, Barcelona.
- ARMERO, F. & GARIKIPATI, K. [1996] "An Analysis of Strong Discontinuities in Multiplicative Finite Strain Plasticity and their Relation with the Numerical Simulation of Strain Localization in Solids," *Int. J. Solids and Structures*, **33**, 2863-2885.
- ASARO, R.J. [1983] "Micromechanics of Crystals and Polycrystals," in *Advances in Applied Mechanics*, **23**, 1-115.
- BAI, Y. & DODD, B. [1992] *Adiabatic Shear Localization; Occurrence, Theories and Localization*, Pergamon Press, Oxford.
- BAZANT, Z.P.; BELYTSCHKO, M. & CHANG, T.P. [1984] "Continuum Theory for Strain-Softening", *J. Eng. Mech., ASCE*, **110**, 1666-1691.

- BAZANT, Z. & BELYTSCHKO, T. [1985] "Wave Propagation in a Strain Softening Bar," *ASCE J. Eng. Mech.*, **111**, 381-389.
- BAZANT & OH [1983] "Crack Band Theory for Fracture of Concrete," *Materials and Structures*, RILEM, **16**, 155-177.
- BELYRSCHKO, T.; FISH, J. & ENGELMANN, B.E. [1988] "A Finite Element with Embedded Localization Zones," *Comp. Meth. Appl. Mech. Eng.*, **70**, 59-89.
- BELYTSCHKO, T.; MORAN, B. & KULKARNI M. [1991] "On the Crucial Role of Imperfections in Quasi-Static Viscoplastic Solutions," *Journal of Applied Mechanics*, **58**, 658-665.
- DEBORST, R. & SLUYS, L.J. [1991] "Localization in a Cosserat Continuum under Static and Loading Conditions", *Comp. Meth. Appl. Mech. Eng.*, **90**, 805-827.
- COLEMAN, B.D. & HODGON, M.L. [1985] "On Shear Bands in Ductile Materials", *Arch. Rat. Mech. Anal.*, **90**, 219-247.
- CROUZEIX, M. & RAVIART, P.A. [1973] "Conforming and nonconforming finite element methods for solving the stationary Stokes equations", *R.A.I.R.O. Anal. Numer.*, **7**, 33-76.
- DVORKIN, E.; CUITIÑO, A. & GOIA, G. [1990] "Finite Elements with Displacement Interpolated Embedded Localization Lines Insensitive to Mesh and Distortions," *Int. J. Num. Meth. Eng.*, **30**, 541-564.
- HILL, R. [1950] *The Mathematical Theory of Plasticity*, Clarendon Press, Oxford.
- HILL, R. [1962] "Acceleration Waves in Solids," *J. Mech. Phys. Solids*, **16**, 1-10.
- HILLERBORG, A.; MODEER, M. & PETERSSON, P. [1976] "Analysis of Crack Formation and Crack Growth in Concrete by Means of Fracture Mechanics and Finite Elements," *Cement and Concrete Research*, **6**, 773-782.
- PIJAUDIER-CABOT, G.; BODE, L. & HUERTA, A. [1995] "Arbitrary Lagrangian-Eulerian Finite Element Analysis of Strain Localization in Transient Problems," *Int. J. Numer. Meth. Eng.*, **38**, 4171-4191.
- JOHNSON, C. [1976] "Existence Theorems for Plasticity Problems," *J. Math. Pures et Appliq.* **55**, 431-444.
- LARSSON, R. & RUNESSON, K. [1996] "Element Embedded Localization Band Based on Regularized Displacement Discontinuity", *J. Eng. Mech.*, **122**, 402-411.
- LAURSEN, T.A. [1994] "The Convected Description in Large Deformation Frictional Contact Problems," *Int. J. Solids Structures*, **31**, 669-681.
- LEROY, Y. & ORTIZ, M. [1990] "Finite Element Analysis of Transient Strain Localization

- Phenomena in Frictional Solids”, *Int. J. Numer. Analyt. Meth. Geom.*, **14**, 93-124.
- LUBLINER, J. [1990] *Plasticity Theory*, Macmillan Publishing Company, New York.
- MANDEL, J. [1966] “Conditions de Stabilité et Postulat de Drucker”, in *Rheology and Soli Mechanics*, IUTAM Symposium, Grenoble 1964, ed. by J. Kravtchenko and P.M. Sirieys, 58-68.
- MATTHIES, H.; STRANG, G. & CHRISTIANSEN, E. [1979] “The Saddle Point of a Differential Program,” in *Energy Methods in Finite Element Analyses*, edited by Glowinski, Rodin & Zienkiewicz, John Wiley & Sons, London.
- MOLINARI, A. & CLIFTON, R.J. [1987] “Analytical Characterization of Shear Localization in Thermoviscoplastic Materials,” *Journal of Applied Mechanics*, **54**, 806-812.
- MÜHLHAUS, H.B. & VARDOULAKIS, I. [1987] “The Thickness of Shear-Bands in Granular Materials,” *Geotechnique*, **35**, 299-317.
- NACAR, A.; NEEDLEMAN, A. & ORIZ, M. [1989] “A Finite Element Method for Analyzing Localization in Rate Dependent Solids at Finite Strains,” *Comp. Meth. Appl. Mech. Eng.*, **73**, 235-258.
- NEEDLEMAN, A. [1988] “Material Rate Dependence and Mesh Sensitivity in Localization Problems,” *Comp. Meth. Appl. Mech. Eng.*, **67**, 69-85.
- NEEDLEMAN, A. & TVERGAARD, V. [1984] “Finite Element Analysis of Localization in Plasticity,” in *Finite Elements. Special Problems in Solid Mechanics*, Volume V, ed. by J.T. Oden and G.F. Carey, Prentice Hall, Englewood Cliffs.
- NEILSEN, M.K. & SCHREYER, H.L. [1993] “Bifurcation in Elastic-Plastic Materials,” *Int. J. Solids Struct.*, **30**, 521-544.
- OLIVER, J. [1989] “A Consistent Characteristic Length for Smearred Cracking Problems”, *Int. J. Num. Meth. Eng.*, **28**, 461-474.
- OLIVER, J. [1996] “Modelling Strong Discontinuities in Solid Mechanics via Strain Softening Constitutive Equations. Part 1: Fundamentals. Part 2: Numerical Simulation,” *Int. J. Num. Meth. Eng.*, **39**, 3575-3623.
- ORTIZ, M.; LEROY, Y. & NEEDLEMAN, A. [1987] “A Finite Element Method for Localized Failure Analysis,” *Comp. Meth. Appl. Mech. Eng.*, **61**, 189-214.
- OTTOSEN, N.S. & RUNESSON, K. [1991] “Properties of Discontinuous Bifurcation Solutions in Elasto-Plasticity,” *Int. J. Solids Struct.*, **27**, 401-421.
- PIETRUSZCZAK, ST. & MRÓZ, Z. [1981] “Finite Element Analysis of Deformation of Strain-Softening Materials,” *Int. J. Numer. Meth. Eng.*, **17**, 327-334.
- PRANDTL, L. [1920] “Ueber die Haerte Plastischer Koerper,” *Goettinger Nachrichten*,

74-84.

- READ, H.E. & HEGEMEIER, G.A. [1984] "Strain Softening of Rock, Soil and Concrete; a Review Article," *Mechanics of Materials*, **3**, 271-294.
- RICE, J. [1976] "The Localization of Plastic Deformations", in *Theoretical and Applied Mechanics*, ed. by W.T. Koiter, 207-219.
- ROTS, J.G.; NAUTA, P.; KUSTERS, G. & BLAAUWENDRAA, T. [1985] "Smearred Crack Approach and Fracture Localization in Concrete," *Heron*, **30**.
- SIMO, J.C. [1992] "Algorithms for Multiplicative Plasticity that Preserve the Form of the Return Mappings of the Infinitesimal Theory," *Comp. Meth. Appl. Mech. Eng.* **99**, pp.61-112.
- SIMO, J.C. & HUGHES, T.J.R. [1997] *Plasticity and Viscoplasticity, Formulation and Numerical Analysis*, Springer Verlag, preprint.
- SIMO, J.C.; OLIVER, J. & ARMERO, F. [1993] "An Analysis of Strong Discontinuities Induced by Softening Solutions in Rate Independent Solids," *J. Comput. Mech.*, **12**, 277-296.
- SIMO, J.C. & RIFAI, S. [1990] "A Class of Mixed Assumed Strain Methods and the Method of Incompatible Modes," *Int. J. Num. Meth. Eng.*, **29**, 1595-1638.
- SLUYS, L.J. [1992] "Wave Propagation, Localisation and Dispersion in Softening Solids" Ph.D. Dissertation, Delft Technological University, The Netherlands.
- STAKGOLD, I. [1979] *Green's Functions and Boundary Value Problems*, Wiley, New York.
- SUQUET, P.M. [1981] "Sur les Equations de la Plasticité: Existence et Régularité des Solutions," *Journal de Mécanique*, **20**, 3-39.
- TEMAM, R. [1984] *Mathematical Problems in Plasticity*, Gauthier-Villars, Paris.
- THOMAS, T.Y. [1961] *Plastic Flow and Fracture in Solids*, Academic Press.
- TRUESDELL & NOLL [1965] "The Nonlinear Field Theories of Mechanics," *Handbich der Physik Bd. III/3*, ed. by S. Fluegge, Springer Verlag, Berlin.
- TVERGAARD, V.; NEEDLEMAN, A. & LO, K.K. [1981] "Flow Localization in the Plane Strain Tensile Test," *Jour. Mech. Phys. Solids*, **29**, 115-142.
- VARDOULAKIS, I. [1979] "Formataion of Shear Bands in Sand Bodies as a Bifurcation Problem," *Int. J.* , **32**, 35-54.